fibers

MDPI

Article

Valorization of Recycled Textile Fibers from Moroccan Industrial Waste for Cementitious Composites: A Multi-Level Experimental Investigation

Ikrame Hattab [1], Otmane Boudouch [2], Amine Naim [3] and Reda Elkacmi [1,*]

[1] Laboratory of Environmental, Ecological and Agro-Industrial Engineering, Faculty of Science and Technology, Sultan Moulay Slimane University, BP 592, Beni-Mellal 23000, Morocco; hattab.ikrame@usms.ac.ma
[2] Laboratory of Sciences and Technologies Team, Higher Education and Training School, Chouaib Doukkali University, BP 299, El Jadida 24000, Morocco; oboudouch@gmail.com
[3] Laboratory of Physico-Chemical Sciences, Faculty of Sciences FS Ben M'Sik, Hassan II University, BP 7955, Casablanca 20670, Morocco; aminaim@gmail.com
* Correspondence: r.elkacmi@usms.ma

Highlights

What are the main findings?

- Recycled polypropylene (PP) fibers from Moroccan industrial textile waste were successfully incorporated as reinforcement in cementitious composites.
- A systematic, multi-scale screening methodology was established to select representative fibers from a highly heterogeneous industrial waste stream, identifying four distinct fiber types.
- Fiber incorporation significantly reduced early-age shrinkage by up to 75% compared to reference mixtures, representing the most pronounced beneficial effect.
- The influence on compressive strength was significant and depended on a strong interaction between fiber type and dosage ($p < 0.001$), while flexural strength showed a favorable but statistically non-significant numerical increase of up to 8.2%.
- Selected formulations exhibited favorable transport-related durability indicators after 90 days of curing, including low chloride diffusion, water-accessible porosity, and gas permeability, with F8B2 showing the most balanced performance.

What is the implication of the main findings?

- This study provides a practical framework for valorizing challenging, heterogeneous industrial textile waste, transforming a local waste management challenge into a resource for sustainable construction.
- The demonstrated effectiveness in shrinkage control suggests that recycled PP fibers can mitigate early-age cracking, potentially extending the service life of concrete structures.
- The approach supports circular economy principles by reducing polymer waste and decreasing the demand for virgin materials, offering significant potential for implementation in textile-producing regions.
- The systematic screening protocol developed in this work can serve as a guide for other researchers and industries aiming to incorporate heterogeneous waste streams into cement-based materials.

Check for updates

Academic Editor: Marina Zoccola

Received: 31 July 2026
Revised: 28 August 2026
Accepted: 31 August 2026
Published: 3 September 2026

Copyright: © 2026 by the authors. Licensee MDPI, Basel, Switzerland. This article is an open access article distributed under the terms and conditions of the Creative Commons Attribution (CC BY) license.

Abstract

The valorization of industrial textile waste as reinforcement in cementitious materials offers a promising approach for reducing polymer waste while improving the performance of

cement-based composites. This study investigates recycled polypropylene (PP) fibers recovered from Moroccan pre-consumer textile waste for application in mortar and concrete. Thirteen fiber types were initially screened based on their geometrical and morphological characteristics, and four representative fibers were selected for detailed characterization and experimental evaluation. Fiber-reinforced mortars were first investigated to assess the influence of fiber type and dosage, followed by concrete-scale evaluation through mechanical, shrinkage, transport-related, and microstructural tests. The results showed that fiber characteristics and dosage influenced composite performance, with the magnitude and direction of the mechanical response depending on the fiber formulation. Statistical analysis confirmed that compressive strength was significantly affected by fiber type, dosage, and their interaction, whereas no statistically significant effect was detected for flexural strength at the 95% confidence level. The F8 mixture containing 0.10% fibers exhibited the highest compressive strength among the investigated concrete formulations, reaching 28.75 MPa compared with 26.25 MPa for the reference concrete. Flexural strength showed numerical increases of up to 8.2% for selected formulations, although these differences were not statistically significant. Early-age shrinkage was reduced by up to 75% compared with the reference mixtures, representing the most pronounced effect observed in the study. Increasing fiber content reduced workability and promoted fiber agglomeration, highlighting the importance of controlled dosage and dispersion. Among the investigated dosage levels, 0.10% by mass of cement was selected for subsequent durability and microstructural investigations because it provided a favorable overall balance among the evaluated properties for the selected formulations; this dosage should not be interpreted as a universal optimum. The F8 formulation exhibited favorable transport-related properties after 90 days of water curing, while SEM observations indicated a generally homogeneous fiber distribution within the investigated regions. Overall, the results demonstrate the potential of heterogeneous recycled PP textile fibers as reinforcement for cementitious composites under the investigated conditions and provide a systematic multi-scale experimental workflow for their screening and evaluation.

Keywords: recycled polypropylene fibers; textile waste valorization; fiber-reinforced concrete; cementitious composites; shrinkage; durability; sustainable construction; circular economy

1. Introduction

Concrete is one of the most widely used construction materials worldwide, but its performance is still limited by its intrinsically low tensile strength and brittle fracture behavior, which can lead to crack initiation and propagation, particularly under restrained shrinkage and early-age deformation [1–3]. Controlling such cracking is therefore a major engineering challenge in cement-based materials, especially for applications such as slabs-on-grade, precast concrete elements, pavements, and thin shell structures. In this context, fiber reinforcement has emerged as an effective approach to improve crack control and post-cracking performance without fundamentally modifying the conventional concrete matrix [3,4].

To address these challenges, fiber-reinforced cementitious composites (FRCC) have been extensively investigated over the past decades. Among the various reinforcing fibers, polypropylene (PP) fibers have gained widespread acceptance owing to their low density, chemical inertness, corrosion resistance, and cost-effectiveness [5]. Their ability to control plastic shrinkage cracking, improve post-cracking ductility, enhance energy absorption, and contribute to the mechanical and durability performance of concrete has been extensively

demonstrated [5–8]. Recent studies have also reported the potential of polypropylene fibers to improve flexural performance, frost resistance, abrasion resistance, and resistance to aggressive environments, highlighting their multifunctional role in durable concrete applications [9,10]. In recent years, increasing attention has also been devoted to recycled polymeric fibers as potential alternatives to virgin synthetic fibers, driven by the need to reduce raw material consumption and promote waste valorization [11,12]. Nevertheless, the use of recycled PP fibers originating from real industrial waste streams remains challenging because of their heterogeneous geometry and uncontrolled physical characteristics.

In parallel, the decarbonization of the cement and concrete sector has become an important global priority [13]. At the same time, the valorization of industrial solid waste within circular economy frameworks has emerged as an important research direction in sustainable construction [14,15]. Various industrial by-products, including fly ash and slag-based materials, have been investigated as potential resources for incorporation into cement-based materials, contributing to waste valorization and resource efficiency. In the Moroccan context, untreated electric arc furnace steel slag (EAF-SS) has also recently been investigated as a potential resource for cement-based applications, highlighting opportunities for the valorization of locally generated industrial waste [16]. Similarly, the textile industry generates substantial quantities of pre-consumer and post-consumer textile waste, creating significant challenges for waste management and resource recovery [14,15]. The disposal of these materials through landfilling or incineration can result in the loss of potentially valuable polymeric resources. Consequently, developing high-value applications for textile waste has become an important objective within circular economy strategies. In this context, the recovery and reuse of polypropylene fibers from industrial textile waste could provide an alternative valorization route, while simultaneously reducing the demand for virgin polymeric materials.

Previous studies on recycled polypropylene fibers have mainly investigated fibers obtained from relatively controlled waste streams or commercially processed recycled products, with reported fiber characteristics varying in terms of length, diameter, aspect ratio, and tensile properties [17,18]. For example, Małek et al. [17] investigated recycled polypropylene fibers produced from plastic packaging waste and evaluated their mechanical performance in concrete. Yin et al. [18] investigated recycled PP fibers and compared their performance with virgin PP fibers. These studies have primarily focused on mechanical performance, crack control, and post-cracking behavior, whereas durability-related properties such as freeze–thaw resistance, abrasion resistance, chloride penetration, and long-term post-cracking behavior remain less extensively investigated for recycled PP fibers, particularly when the fibers originate from highly heterogeneous industrial waste streams. In contrast to commercially processed or specifically manufactured recycled fibers, the fibers investigated in the present study originate directly from a Moroccan industrial textile waste stream and exhibit substantial variability in geometry and physical characteristics. This heterogeneity, together with the uncontrolled nature of the industrial waste source, makes the selection of representative fibers and the assessment of their effects on cementitious materials particularly challenging.

Despite this potential, the reuse of industrial textile polypropylene waste as reinforcement in cementitious materials remains insufficiently explored, particularly under real industrial conditions involving heterogeneous fiber geometries and uncontrolled physical characteristics. Most previous studies have focused on recycled fibers with relatively uniform properties or commercially processed recycled products, whereas the behavior of heterogeneous industrial textile waste remains poorly understood [15,17–19]. This limitation is particularly relevant for industrial waste streams, where the objective is not simply

to evaluate a single predefined fiber type, but to establish a rational procedure for screening and selecting representative fibers before their incorporation into cementitious materials.

To address this knowledge gap, the overarching aim of the present study is to evaluate the feasibility of using recycled polypropylene fibers recovered from Moroccan industrial textile waste as reinforcement in mortar and concrete.

To achieve this aim, the study focuses on three main objectives: (i) characterizing the physicochemical, geometrical, and morphological properties of representative recycled PP fibers; (ii) evaluating their effects on fresh-state and mechanical properties; and (iii) investigating their influence on shrinkage, water absorption, and additional durability-related properties at mortar and concrete scales.

The novelty of this study lies in two main contributions. First, it introduces a structured methodology for selecting representative recycled fibers that explicitly accounts for the heterogeneity of real industrial textile waste, thereby establishing a relationship between fiber variability and cementitious performance. Second, it provides an integrated multi-scale experimental dataset, spanning fiber characterization, mortar-scale assessment, and concrete-scale mechanical and durability-related evaluation, using fibers originating directly from a real industrial waste stream under practical production conditions. This approach provides a practical framework for the valorization of heterogeneous industrial textile waste in cement-based materials and supports its potential transfer toward industrial applications.

Accordingly, a multi-scale experimental methodology was adopted through three sequential stages. First, a preliminary screening was performed to identify representative fibers from the heterogeneous industrial waste stream. Second, the selected fibers were subjected to physicochemical, geometrical, and morphological characterization to establish their relevant characteristics. Third, their performance was systematically evaluated through mortar- and concrete-scale experiments, including fresh-state behavior, mechanical performance, shrinkage, water absorption, and additional durability-related properties. This sequential approach was designed to progressively reduce the large variability inherent to the industrial waste stream and to establish a rational link between fiber characteristics, mixture behavior, and cementitious composite performance.

2. Materials and Methods

2.1. Raw Materials

2.1.1. Textile Fiber Waste

Recycled textile fibers were obtained from a Moroccan textile company equipped with an industrial fiber waste treatment unit. The fibers originate from pre-consumer waste generated during cutting and spinning operations. Residual fibers originating from multiple production batches and suppliers were collected in order to capture the heterogeneity encountered within the investigated industrial waste stream. The sampling was designed to include variability in fiber geometry and morphology rather than to provide a statistically exhaustive representation of all seasonal and long-term variations in Moroccan textile production. Accordingly, the selected fiber types should be considered representative of the variability observed within the collected waste stream, while longitudinal sampling over different production periods and seasons would be required to establish broader industrial representativeness.

An initial set of thirteen fiber types was screened based on geometrical properties—primarily fiber length and diameter—which are widely recognized as key parameters governing fiber dispersion and mechanical performance in cementitious composites [17,18]. Fibers exhibiting lengths below 3 mm or unsuitable morphology were excluded, as such fractions fall below the critical embedment length required for effective stress transfer [5,17] and

are known to promote balling effects detrimental to workability [6,7]. This selection step is consistent with established practice in the valorization of heterogeneous recycled fiber feedstocks. Following the preliminary screening, four representative fibers (F1, F2, F5 and F8) exhibiting distinct geometrical characteristics were selected for detailed physicochemical characterization and mechanical evaluation. The selected fibers were subsequently characterized using the following analytical techniques:

- Chemical composition and solvent solubility (NF EN ISO 1833 [20]): (Ventilated oven (GALLI, Milan, Italy) and analytical balance (Mettler Toledo, Greifensee, Switzerland; 220 g capacity, 0.1 mg readability)
- Optical microscopy and cross-sectional morphology analysis:Leica DM2700 optical microscope (Leica Microsystems GmbH, Wetzlar, Germany).
- Fiber diameter and length measurements:Leica DM2700 optical microscope (Leica Microsystems GmbH, Wetzlar, Germany).
- Linear density (dtex):Leica DM2700 optical microscope (Leica Microsystems GmbH, Wetzlar, Germany) and analytical balance (Mettler Toledo, Greifensee, Switzerland; 220 g capacity, 0.1 mg readability).
- Combustion test and melting point determination:: differential scanning calorimeter (DSC 3, Mettler-Toledo, Greifensee, Switzerland).
- Density measurement:: analytical balance (Mettler Toledo, Greifensee, Switzerland; 220 g capacity, 0.1 mg readability).

2.1.2. Cement and Aggregates

The cementitious matrix was prepared using Portland composite cement (CPJ 45) (Holcim Maroc, Casablanca, Morocco). Aggregates included sea sand (0/2), crushed sand (0/5), and crushed gravel (GI: 6.3/16 mm and GII: 14/20 mm) (quarry in the Benslimane region, Morocco). Potable water was used for all mixtures. All aggregates were characterized according to standard procedures; the main physical and mechanical properties are summarized in Table 1.

Table 1. Physical and mechanical properties of aggregates.

Property	Sea Sand	Crushed Sand	Gravel GI	Gravel GII
Particle Size class	0/2	0/5	6.3/16	14/20
Fineness modulus	1.06	3.01	-	-
Fines Content (%)	0.8	11.7	-	-
Sand Equivalent (%)	80	72	-	-
Methylene blue (g/kg)	0.5	0.7	-	-
Bulk density (t/m^3)	1.53	1.69	1.43	1.48
True density (t/m^3)	2.78	2.72	2.65	2.74
Water absorption (%)	0.65	0.65	0.55	0.53
Los Angelos (%)	-	-	19	16

The combined grading of the aggregates complied with the recommended particle size distribution for concrete production, ensuring adequate packing density, satisfactory workability, and reduced void content.

2.2. Experimental Program

The overall experimental methodology adopted in this study is schematically illustrated in Figure 1. The workflow comprises four successive stages: (i) collection and

preliminary screening of recycled textile fibers, (ii) physicochemical characterization of the selected fibers, (iii) mortar-scale optimization, and (iv) evaluation of the selected dosage through concrete mechanical and durability assessments.



Figure 1. Schematic overview of the experimental methodology adopted in this study, from recycled textile fiber selection and characterization to mortar -scale screening and concrete performance evaluation.

The experimental program was designed according to a hierarchical, multi-criteria screening approach. Mortar-scale tests were first used to identify the most suitable recycled textile fibers and dosages based on compressive and flexural strength, shrinkage behavior, and observations of workability and fiber dispersion during mixing. The resulting performance

trends were then used to select the formulations for concrete-scale validation. This sequential procedure allowed the number of concrete mixtures to be limited while ensuring that the most promising combinations of fiber type and dosage were evaluated at the concrete scale.

2.2.1. Mortar Preparation

Mortar mixtures were prepared with a cement:sand:water ratio of 1:3:0.5 under controlled laboratory conditions (20 ± 2 °C; relative humidity ≥ 50%). The selected fibers were incorporated at fiber contents ranging from 0.05% to 0.50% by mass of cement, consistent with commonly reported ranges for PP fiber-reinforced mortars [17,21].

Mixing was performed mechanically(Mechanical mixer: Beratest, Oberentfelden, Switzerland): dry materials were first combined for 1 min, followed by water addition and mixing for 2 additional minutes. Fibers were then gradually introduced to promote homogeneous dispersion. Prismatic specimens (40 × 40 × 160 mm) were cast and compacted using a jolting table (Beratest, Oberentfelden, Switzerland). After 24 h, the specimens were demolded, and the initial reference length was determined using an extensometer (Matest, Treviolo, Italy) in accordance with NM 10.0.005 [22]. The specimens were then immersed in water at 20 ± 1 °C until the corresponding measurement ages. Total dimensional variation (total shrinkage) was measured at 2, 3, 5, and 7 days, with measurements performed on specimens for each mixture. The reported shrinkage values therefore represent the total dimensional variation measured under the specified curing conditions and should not be interpreted as drying or autogenous shrinkage separately.

2.2.2. Concrete Preparation

Concrete mixtures were designed using the Dreux–Gorisse method to optimize particle packing and achieve the required mechanical performance while maintaining adequate workability [23,24]. A reference composition was established, and all mix proportions other than fiber dosage were kept constant throughout the study. The mortar-scale results were used as a preliminary multi-criteria screening step to identify the most promising fiber types and dosages based on mechanical performance, shrinkage behavior, and visual observations of fiber dispersion. The higher dosages investigated at the mortar scale (0.30% and 0.50%) generally resulted in lower compressive strength compared with the reference mixture and the lower dosages (0.05–0.10%), with the reductions being particularly pronounced for some fiber types. Based on these results and the observed fiber dispersion, the concrete-scale investigation was restricted to dosages up to 0.15%. In addition, a dosage of 0.15% was introduced as an intermediate level between 0.10% and 0.30% to explore the upper boundary of the selected dosage range under actual concrete conditions. The final concrete dosages were therefore 0.05%, 0.10%, and 0.15%. The reference concrete mix proportions are presented in Table 2.

Table 2. Concrete Mix proportions (kg/m^3).

Sample Code	Quantity (Kg/m^3)
Cement	373
Water	205
Sea sand (0/2)	162
Crushed sand (0/5)	735
Gravel GI	368
Gravel GII	720
Water/Cement ratio	0.55

The reference mixture was designed to provide adequate workability while maintaining a constant water-to-cement ratio (0.55) throughout the study, thereby allowing the influence of fiber characteristics and dosage to be isolated.

Fiber dosages of 0.05%, 0.10%, and 0.15% by mass of cement were incorporated, corresponding to 0.19, 0.37, and 0.56 kg/m^3, respectively. Fresh concrete workability was evaluated using the slump test (NM 10.1.061) [25]. Hardened properties were assessed through compressive strength (NM 10.1.051) [26], flexural strength (NM 10.1.050) [27], shrinkage (NF P 18-427) [28], and water absorption (EN 13369, Annex G) [29].

The concrete mixing procedure(mechanical mixe :(Controlab, Saint-Ouen-l'Aumône, France)) was carried out as follows. First, the cement and aggregates were introduced into the mixer and dry-mixed at low speed. The recycled PP fibers were then added in a single batch to the dry mixture and mixed at low speed for 40 s to promote uniform fiber distribution prior to water addition. The mixer was subsequently stopped, and water was introduced over 20 s. The bowl was then scraped for 15 s to ensure complete incorporation of all constituents. The mixer was operated at high speed for 1 min 15 s, followed by a final mixing phase of 60 s to ensure adequate homogenization and fiber dispersion.

No mechanical or chemical pre-treatment was applied to the fibers prior to incorporation. Fiber de-agglomeration was promoted through the mixing action itself. This mixing sequence was kept consistent for all concrete mixtures to ensure comparable fiber dispersion and experimental conditions.

Shrinkage measurements were performed in accordance with the specified standard procedure, with measurements conducted at 2, 3, 5, and 7 days. The relevant specimen preparation, curing, demolding, measurement procedure, and reference-length determination followed the requirements of the applicable standard.

Prismatic specimens with dimensions of 100 × 100 × 400 mm were used for flexural strength testing, while prismatic specimens with dimensions of 70 × 70 × 280 mm were used for shrinkage measurements. For compressive strength testing, cylindrical specimens with a diameter of 160 mm and a height of 320 mm were used. Cubic specimens (100 × 100 × 100 mm) were used for water absorption. Water absorption was determined in accordance with EN 13369 (Annex G) by immersing the specimens in water until constant saturated mass (M_1), followed by oven drying at 105 ± 5 °C until constant dry mass (M_2):

$$\text{Absorption (\%)} = (M_1 - M_2)/M_2 \times 100$$

All experimental measurements were performed in triplicate. The reported results correspond to the mean values, while the associated standard deviations were calculated to evaluate experimental variability.

2.2.3. Scanning Electron Microscopy (SEM-EDS)

To investigate the morphology of the recycled textile fibers and the microstructure of the fiber-reinforced concrete, Scanning Electron Microscopy coupled with Energy Dispersive X-ray Spectroscopy (SEM–EDS) was employed. The analyses were carried out using a scanning electron microscope (JEOL Ltd., Akishima, Tokyo, Japan) equipped with an EDS detector(Oxford Instruments, High Wycombe, United Kingdom) under high-vacuum conditions at an accelerating voltage of 15 kV.

Prior to concrete production, SEM observations were performed on the recycled textile fibers to examine their surface morphology and filament arrangement. After curing, SEM was used to investigate the distribution of the fibers within the cementitious matrix and to qualitatively assess the morphology of the hardened composite.

EDS analysis was performed on selected regions to determine their elemental composition through the detection of characteristic X-rays emitted during the interaction between the electron beam and the specimen. This non-destructive microanalytical technique provides complementary information on both the morphology and the elemental composition of the investigated materials [30].

Based on the overall experimental results, including mechanical performance and durability, the F8B2 concrete mixture, reinforced with 0.10% (by mass of cement) F8 recycled polypropylene textile fibers, was selected for SEM–EDS characterization. Both the recycled fibers and the selected concrete mixture were analyzed in order to investigate fiber morphology, fiber distribution within the cementitious matrix, and the elemental composition of the analyzed regions.

2.2.4. Durability Tests

To evaluate transport-related durability indicators of the investigated concrete mixtures at 90 days. The apparent chloride diffusion coefficient was determined according to XP P18-462 [31], the water-accessible porosity according to NM 10.1.658 [32], and the apparent gas permeability according to NM 10.1.442 [33]. These tests were conducted to assess the resistance of the developed concretes to the penetration and transport of aggressive agents.

2.2.5. Statistical Analysis

Statistical analyses were performed using the three individual measurements obtained for each concrete formulation. The results are reported as mean ± standard deviation. One-way analysis of variance (ANOVA) was initially performed to determine whether the concrete formulation significantly affected the 28-day compressive and flexural strengths. The concrete formulation was considered as a categorical factor, including the control mixture and all investigated fiber-reinforced mixtures(R software, version 4.5.1, R Foundation for Statistical Computing, Vienna, Austria).

To further assess the individual and combined effects of fiber characteristics, a two-way ANOVA was performed on the fiber-reinforced concrete mixtures, considering fiber type (F1, F2, F5, and F8) and fiber dosage (0.05%, 0.10%, and 0.15% by mass of cement) as fixed factors. The interaction between fiber type and dosage was also evaluated. Separate analyses were conducted for compressive and flexural strength at 28 days.

When the one-way ANOVA indicated a statistically significant difference among formulations, Tukey's honestly significant difference (HSD) post hoc test was used for pairwise comparisons. Statistical significance was assessed at a 95% confidence level ($\alpha = 0.05$). Thus, differences were considered statistically significant when $p < 0.05$.

3. Results and Discussion

3.1. Fiber Screening and Selection

An initial set of thirteen fiber types was subjected to preliminary morphological screening. Fibers with lengths below 3 mm or presenting handling difficulties during mixing trials were excluded. The selection procedure applied a multi-criteria screening approach based on fiber length, diameter, cross-sectional morphology, and processability. Four representative fibers (F1, F2, F5, and F8) were retained because they exhibited distinct combinations of these characteristics and collectively spanned the main range of geometrical and morphological variability observed in the waste stream. The selected fibers ranged from fine, uniform cylindrical filaments (F1) to fibers exhibiting mixed and irregular cross-sectional morphologies (F5).

3.2. Fiber Characterization

3.2.1. Morphological Analysis

The morphological characterization of the recycled fibers was performed by qualitative optical microscopy according to an internal laboratory method. Several fibers were sampled from each investigated lot and mounted on glass slides using an alcohol–glycerin (50/50)

medium before microscopic observation. The examination focused on the main morphological characteristics, including fiber shape, surface features, and cross-sectional morphology.

Optical microscopy showed that recycled fibers are predominantly multi-filament polypropylene structures with mainly cylindrical morphology. Heterogeneous geometries were also observed, including hollow and triangular cross-sections in F5, reflecting the mechanical shredding origin of the waste stream. Fiber lengths ranged from 3 to 24 mm, confirming the high variability typical of industrial textile waste. Such heterogeneity may influence dispersion behavior and fiber–matrix interaction in cementitious composites [17,18].

The initial set of thirteen fiber types was reduced to four representative fibers through a two-stage screening process. In the first stage, fibers exhibiting lengths below 3 mm were excluded on the basis of insufficient embedment length for effective stress transfer and workability preservation. In the second stage, the remaining fiber types were subjected to preliminary mortar-scale and concrete-scale trials assessing mechanical behavior. The four retained fibers—F1, F2, F5, and F8—consistently produced interpretable and reproducible results across all investigated parameters, while representing the widest range of geometrical and morphological variability observed among the processable fiber types. The complete characterization data for all thirteen initial fiber types, including their selection status and reasons for exclusion, are provided in Supplementary Table S1.

3.2.2. Chemical Composition and Solubility

Solubility tests in hot xylene confirmed the thermoplastic nature of all fibers. Chemical composition analysis further confirmed that all selected fibers consisted of 100% polypropylene. Thus, differences in polymer chemistry were minimized among the selected fibers, providing a consistent basis for comparing their performance in cementitious matrices.

However, despite their common polypropylene composition, the recycled fibers exhibited differences in surface morphology, filament structure, cross-sectional geometry, and physical condition resulting from the recycling process. These characteristics, together with the quality of fiber dispersion during mixing, may influence fiber–matrix interaction and consequently the mechanical and shrinkage behavior of the composites [17,18]. Therefore, the observed differences in performance cannot be attributed exclusively to fiber geometry, but rather to the combined effects of geometrical, morphological, and dispersion-related characteristics.

3.2.3. Geometrical Properties

The geometrical characteristics of the selected recycled textile fibers are summarized in Table 3 and Figure 2. Fiber diameters ranged from 19.6 μm (F1) to 37.0 μm (F8), fiber lengths varied between 6 and 12 mm, and linear density ranged from 2.72 to 9.68 dtex. These diameter values fall within the typical range reported for polypropylene fibers used in cementitious composites (15–50 μm) [7,17], indicating that the recycled fibers possess geometrical characteristics suitable for cement-based materials. The resulting aspect ratios (length-to-diameter) ranged from approximately 162 (F8) to 361 (F2), reflecting substantial variability among the selected fibers despite their common polymeric origin. Although most fibers exhibited a circular cross-section consistent with the spinneret die geometry, F5 presented a heterogeneous morphology composed of circular, hollow, and triangular filaments. Such differences in cross-sectional geometry and aspect ratio may influence fiber–matrix interfacial interaction, mechanical anchorage, dispersion, and crack-bridging efficiency. These effects may also be influenced by surface roughness, filament arrangement, and the physical condition of the recycled fibers resulting from the recycling process [17,18]. However, these geometrical parameters should be considered together

with surface morphology, fiber structure, and dispersion quality, which may also affect fiber–matrix interaction and composite performance.

Table 3. Geometric characteristics of the selected fibers.

Fiber	Cross Section	Diameter (μm)	Length (mm)	Aspect Ratio (L/D)	Linear Density (dtex)
F1	Circular	19.6	6	306	2.72
F2	Circular	33.2	12	361	7.79
F5	Mixed (circular, hollow, triangular)	33.8	6	178	8.08
F8	Circular	37.0	6	162	9.68

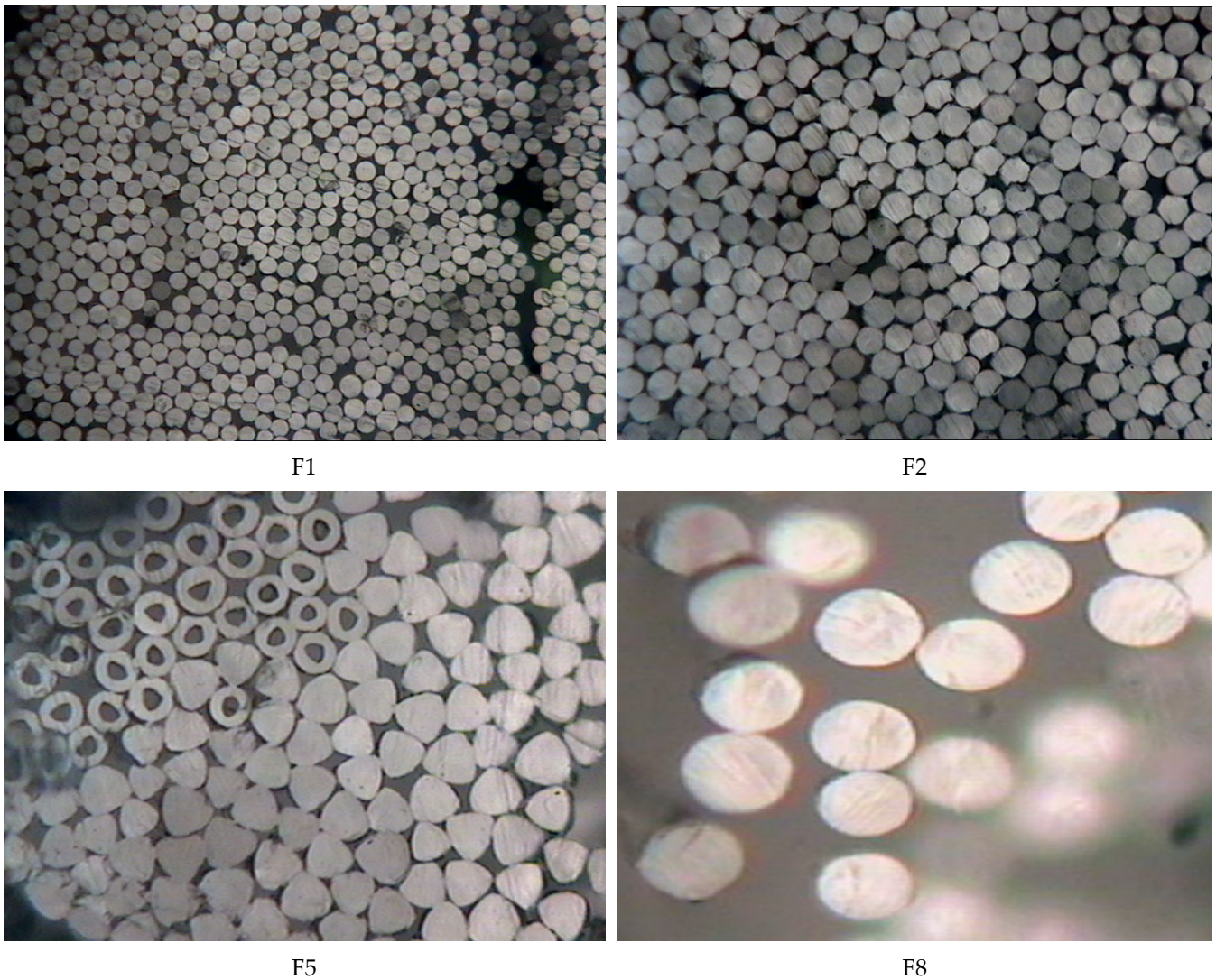

Figure 2. Cross sections of the selected fibers.

3.2.4. Physical Properties

All fibers exhibited typical polypropylene thermal behavior, including softening, melting between 150 and 160 °C, curling, and droplet formation during combustion. These observations are consistent with the thermal behavior generally associated with polypropylene [34]. Density values were highly uniform (0.89–0.90 g/cm^3), confirming the lightweight nature of the recycled PP fibers. The relatively low and uniform density may facilitate their

incorporation into cementitious matrices; however, fiber dispersion is also influenced by other factors, including fiber geometry, surface morphology, multifilament structure, and mixing conditions [7,17]. Physical properties are summarized in Table 4.

Table 4. Physical properties of the selected fibers.

Fiber	Melting Point (°C)	Density (g/cm^3)	Filament Type
F1	160	0.89	Multi-filament
F2	160	0.90	Multi-filament
F5	145/160	0.90	Multi-filament
F8	160	0.90	Multi-filament

3.3. Mortar Scale Results

3.3.1. Mechanical Performance

Compressive and flexural strength results for all fiber-reinforced mortar mixtures at 2, 7, and 28 days are presented in Table 5 and Figure 3. The incorporation of recycled PP fibers had a limited influence on compressive strength at low fiber dosages (0.05–0.10%), whereas more pronounced reductions were observed at higher dosages (0.30–0.50%), particularly for F1, F5, and F8. These reductions may be associated with increased air entrapment and local fiber agglomeration during mixing, potentially resulting from changes in mixture consistency at higher fiber dosages. The observed behavior may also depend on fiber morphology, filament arrangement, surface characteristics, and dispersion quality within the mortar matrix [35,36].

Table 5. Compressive (MPa) and flexural (MPa) strength of fiber-reinforced mortars at 2, 7, and 28 days.

e	Dosage	Flex. 2 d	Flex. 7 d	Flex. 28 d	Comp. 2 d	Comp. 7 d	Comp. 28 d
Control	0%	3.57 ± 0.3	5.17 ± 0.4	7.21 ± 0.4	15.52 ± 1	27.18 ± 0.9	40.20 ± 0.8
F1M1	0.05%	3.23 ± 0.2	4.87 ± 0.3	6.83 ± 0.4	14.25 ± 0.8	25.45 ± 0.9	39.89 ± 0.8
F1M2	0.10%	3.37 ± 0.2	5.00 ± 0.3	7.34 ± 0.4	14.87 ± 0.9	26.97 ± 0.7	40.16 ± 0.8
F1M3	0.30%	3.40 ± 0.2	4.93 ± 0.4	6.49 ± 0.3	13.98 ± 0.9	26.08 ± 0.7	36.89 ± 0.8
F1M4	0.50%	2.93 ± 0.15	4.17 ± 0.3	6.30 ± 0.4	12.67 ± 0.9	22.57 ± 0.7	33.67 ± 0.9
F2M1	0.05%	3.63 ± 0.3	5.53 ± 0.4	7.40 ± 0.4	15.75 ± 0.9	28.43 ± 0.8	43.25 ± 0.9
F2M2	0.10%	3.47 ± 0.3	5.33 ± 0.4	7.31 ± 0.4	15.27 ± 0.9	28.23 ± 0.8	40.68 ± 0.9
F2M3	0.30%	3.10 ± 0.2	5.27 ± 0.4	7.36 ± 0.4	13.82 ± 0.8	27.45 ± 0.8	38.04 ± 0.9
F2M4	0.50%	3.20 ± 0.2	5.07 ± 0.4	6.65 ± 0.4	13.20 ± 0.8	23.62 ± 0.8	36.98 ± 0.9
F5M1	0.05%	3.13 ± 0.25	5.30 ± 0.3	7.73 ± 0.5	12.22 ± 0.4	24.42 ± 0.9	38.75 ± 0.9
F5M2	0.10%	3.33 ± 0.2	5.25 ± 0.30	6.73 ± 0.4	12.58 ± 0.5	26.12 ± 0.8	38.52 ± 0.9
F5M3	0.30%	2.50 ± 0.15	4.63 ± 0.3	6.97 ± 0.5	10.62 ± 0.5	21.47 ± 0.9	34.02 ± 0.9
F5M4	0.50%	2.43 ± 0.15	4.13 ± 0.4	6.93 ± 0.5	10.20 ± 0.5	18.65 ± 0.6	32.32 ± 0.9
F8M1	0.05%	3.20 ± 0.25	4.83 ± 0.3	6.67 ± 0.4	9.72 ± 0.5	22.10 ± 0.6	35.23 ± 0.9
F8M2	0.10%	3.60 ± 0.30	5.57 ± 0.4	6.80 ± 0.4	10.82 ± 0.5	26.52 ± 0.6	37.77 ± 0.9
F8M3	0.30%	3.40 ± 0.30	4.70 ± 0.4	6.53 ± 0.40	11.55 ± 0.4	22.85 ± 0.6	35.18 ± 0.9
F8M4	0.50%	3.50 ± 0.30	4.47 ± 0.4	6.47 ± 0.4	9.60 ± 0.4	19.62 ± 0.5	35.02 ± 0.9

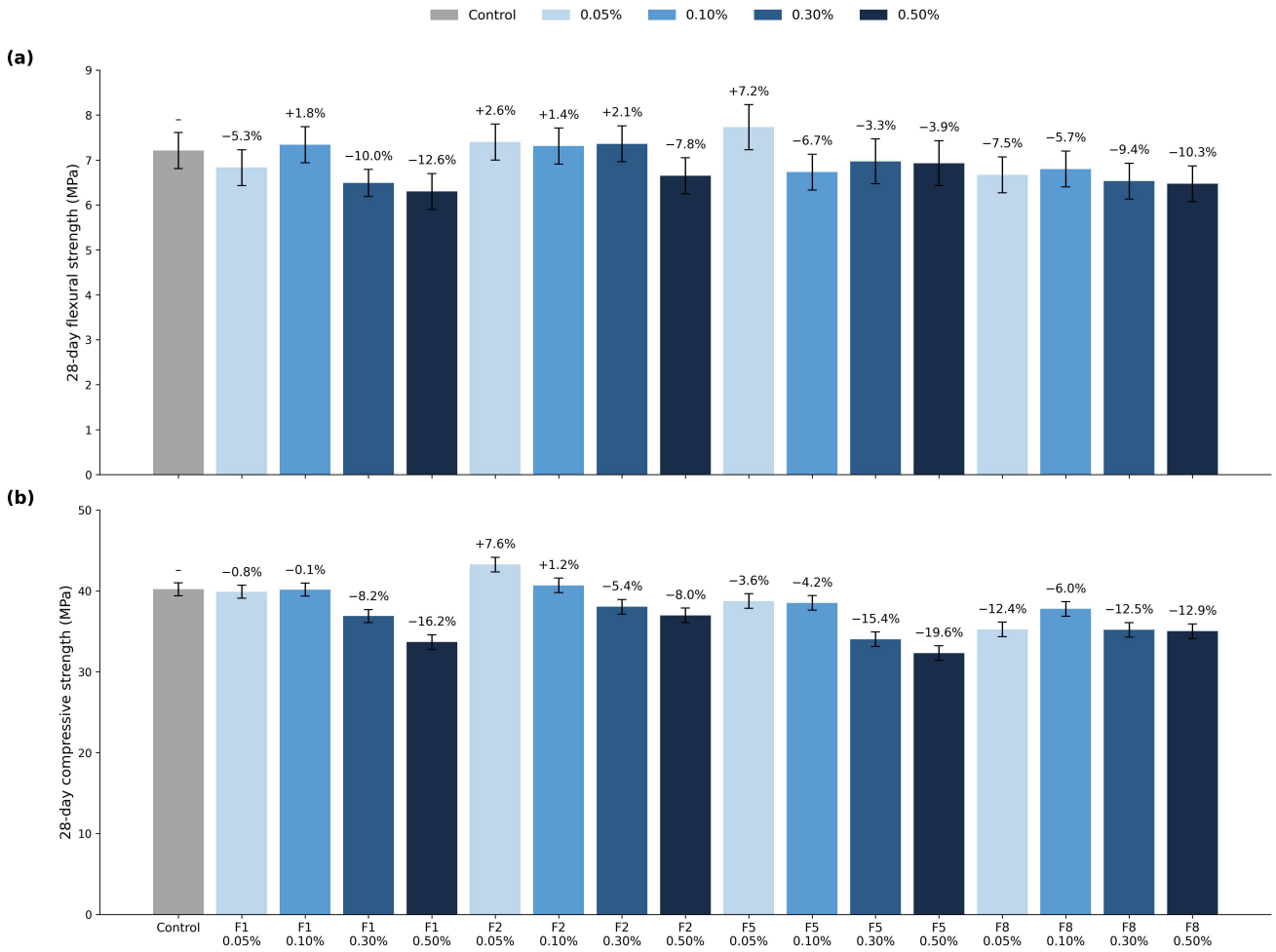

Figure 3. (**a**) Flexural and (**b**) compressive strength of concrete mixes at 28 days. Error bars represent standard deviation; percentages indicate variation relative to Control.

In contrast, flexural performance was enhanced at selected fiber dosages. At 28 days, flexural strength reached up to 7.73 MPa (F5M1), representing an approximately 7.2% improvement over the control (7.21 MPa), which is consistent with the expected crack-bridging contribution of the recycled fibers [5,7,17,18]. The magnitude of this improvement varied among fiber types, suggesting that fiber geometry and morphology, together with dispersion quality and fiber–matrix interaction, may contribute to the observed differences in flexural performance [7,35,37].

3.3.2. Shrinkage Behavior

All fiber-reinforced mortars exhibited a significant reduction in early-age shrinkage compared to the control mixture (217 μm/m at 3 days). Results are presented in Table 6. The maximum reduction reached approximately 60–75% depending on fiber type and dosage. Among the investigated mortar dosages, F2 at 0.50% achieved the lowest value (56 μm/m), corresponding to a 74.2% reduction. This improvement may be attributed to the formation of a three-dimensional fiber network restraining volumetric deformation during cement hydration [5,18,35,36].

The pronounced reduction in measured total dimensional variation may be associated with the restraining effect of the recycled PP fibers within the cementitious matrix. However, since the present test measures total dimensional variation under the specified curing conditions, the relative contributions of fiber restraint and other moisture-related mechanisms cannot be separated from the present measurements.

Table 6. Early-age shrinkage of fiber-reinforced mortars at 3 days (μm/m).

Fiber	Dosage	Shrinkage at 3 Days (μm/m)
Control	0%	217 ± 5
F1	0.05%	195 ± 5
	0.10%	169 ± 5
	0.30%	140 ± 3
	0.50%	98 ± 3
F2	0.05%	88 ± 3
	0.10%	73 ± 3
	0.30%	69 ± 3
	0.50%	56 ± 3
F5	0.05%	200 ± 8
	0.10%	153 ± 7
	0.30%	132 ± 5
	0.50%	96 ± 5
F8	0.05%	159 ± 6
	0.10%	121 ± 5
	0.30%	111 ± 6
	0.50%	96 ± 6

3.4. Concrete Scale Results

3.4.1. Fresh State Workability

A progressive reduction in slump was observed with increasing fiber content (Table 7). The control mixture achieved a slump of 100 mm; values ranged from 92.5 mm (F1 at 0.05%) to 75.0 mm (F5 and F8 at 0.15%). Despite reduced flowability, mixtures remained cohesive and stable, indicating that fiber addition improves internal cohesion and reduces segregation risk [7,17,35,36].

Table 7. Slump values (mm) of fiber-reinforced concrete mixtures.

Fiber	Dosage	Slump (mm)	Reduction vs. Control
Control	0%	100.0 ± 5	–
F1	0.05%	92.5 ± 5	7.5%
	0.10%	87.5 ± 4	12.5%
	0.15%	85.0 ± 4	15.0%
F2	0.05%	100.0 ± 5	0%
	0.10%	95.0 ± 5	5%
	0.15%	92.5 ± 5	7.5%
F5	0.05%	85.0 ± 4	15%
	0.10%	80.0 ± 4	20%
	0.15%	75.0 ± 4	25%
F8	0.05%	87.5 ± 4	12.5%
	0.10%	80.0 ± 4	20%
	0.15%	75.0 ± 4	25%

A progressive reduction in slump was observed with increasing fiber content (Table 7). The control mixture achieved a slump of 100 mm, while values ranged from 92.5 mm (F1 at 0.05%) to 75.0 mm (F5 and F8 at 0.15%). Despite the reduced flowability, the mixtures remained cohesive and stable, indicating that fiber incorporation may contribute to increased internal cohesion and reduced segregation risk [7,17]. The reduction in slump with increasing fiber content is consistent with findings reported in the literature on fiber-reinforced cementitious systems [17]. This phenomenon may be associated with increased internal friction, the surface characteristics of the fibers, and mechanical interactions between fibers and granular constituents [17]. The extent of the workability reduction may also depend on fiber geometry, surface morphology, fiber dosage, and dispersion quality. The observed reduction in flowability may reflect increased water demand associated with fiber coating and dispersion within the fresh mixture. However, fiber incorporation may enhance mixture cohesion and reduce segregation risk, which can favor more uniform fiber distribution in the hardened state.

3.4.2. Compressive and Flexural Strength

Compressive and flexural strength results for concrete are presented in Table 8. The incorporation of recycled PP fibers produced a formulation-dependent response in compressive strength, with the magnitude and direction of the effect varying according to fiber type and dosage. At 28 days, compressive strength ranged from 25.25 MPa for F2B3 (0.15%) to 28.75 MPa for F8B2 (0.10%), compared with 26.25 MPa for the control concrete. The highest compressive strength was therefore obtained with F8 at 0.10% dosage, whereas the response of the other fiber types was less consistent. For example, F2 exhibited a progressive decrease in compressive strength with increasing dosage, from 26.75 MPa at 0.05% to 25.75 MPa at 0.10% and 25.25 MPa at 0.15%. These results indicate that the effect of fiber dosage cannot be considered independently of fiber type and geometry [35,36,38,39].

Table 8. Compressive and flexural strength (MPa) of fiber-reinforced concrete at 2, 7, and 28 days.

Fiber	Ref.	Dosage	Comp. 2 d (MPa)	Comp. 7 d (MPa)	Comp. 28 d (MPa)	Flex. 2 d (MPa)	Flex. 28 d (MPa)
Control	BN	0%	11.00 ± 0.4	18.00 ± 0.3	26.25 ± 0.5	1.55 ± 0.03	3.65 ± 0.1
F1	F1B1	0.05%	9.25 ± 0.3	17.75 ± 0.3	26.25 ± 0.5	1.55 ± 0.03	3.55 ± 0.1
	F1B2	0.10%	10.30 ± 0.3	18.50 ± 0.3	26.70 ± 0.5	1.65 ± 0.03	3.90 ± 0.2
	F1B3	0.15%	10.15 ± 0.3	18.25 ± 0.3	26.45 ± 0.5	1.55 ± 0.03	3.88 ± 0.2
F2	F2B1	0.05%	12.75 ± 0.5	20.25 ± 0.4	26.75 ± 0.5	1.85 ± 0.02	3.85 ± 0.2
	F2B2	0.10%	11.75 ± 0.4	19.75 ± 0.35	25.75 ± 0.5	1.75 ± 0.02	3.75 ± 0.3
	F2B3	0.15%	10.50 ± 0.3	19.25 ± 0.35	25.25 ± 0.5	1.65 ± 0.03	3.70 ± 0.3
F5	F5B1	0.05%	10.25 ± 0.3	18.25 ± 0.3	25.50 ± 0.5	1.95 ± 0.02	3.85 ± 0.3
	F5B2	0.10%	11.25 ± 0.5	18.75 ± 0.3	27.05 ± 0.6	2.05 ± 0.02	3.95 ± 0.3
	F5B3	0.15%	9.50 ± 0.4	16.90 ± 0.2	26.90 ± 0.6	1.90 ± 0.02	3.90 ± 0.4
F8	F8B1	0.05%	11.25 ± 0.4	18.50 ± 0.3	26.00 ± 0.5	1.65 ± 0.03	3.80 ± 0.3
	F8B2	0.10%	11.75 ± 0.4	20.00 ± 0.4	28.75 ± 0.6	1.80 ± 0.03	3.95 ± 0.4
	F8B3	0.15%	10.75 ± 0.4	18.60 ± 0.4	27.75 ± 0.6	1.65 ± 0.03	3.85 ± 0.3

For flexural strength, several fiber-reinforced mixtures exhibited numerically higher values than the control. The highest 28-day flexural strength was obtained for F5B2 and F8B2 (3.95 MPa), corresponding to an 8.2% numerical increase compared with the control concrete (3.65 MPa). However, the statistical analysis indicated that the differences among

the investigated formulations were not statistically significant (one-way ANOVA, F = 0.565, p = 0.850). Thus, the observed increase in flexural strength should be interpreted as a numerical trend rather than as a statistically confirmed improvement.

For compressive strength, one-way ANOVA showed a statistically significant effect of concrete formulation at 28 days (F = 9.369, $p < 0.001$). A two-way ANOVA performed on the fiber-reinforced mixtures further confirmed significant effects of fiber type (F = 13.689, $p < 0.001$), fiber dosage (F = 9.198, $p = 0.0011$), and their interaction (F = 8.454, $p < 0.001$). The significant fiber type × dosage interaction indicates that the effect of fiber dosage on compressive strength depended on fiber type and therefore could not be generalized across the investigated fiber formulations. Although the 0.10% dosage resulted in the highest compressive strength for F8 (28.75 MPa) and F5 (27.05 MPa), this trend was not consistent across all fiber types. In particular, F2 showed a reduction in compressive strength as the dosage increased from 0.05% to 0.15%. The Tukey HSD post hoc analysis showed that F8B2 was significantly higher than the control concrete ($p < 0.001$), whereas the difference between F8B3 and the control was not statistically significant ($p > 0.05$). Therefore, the results do not support the use of 0.10% as a universal optimum dosage; rather, they indicate that the optimum mechanical response depends on the combination of fiber type, fiber geometry, and dosage.

Overall, the incorporation of recycled PP fibers significantly affected compressive strength, but the effect was formulation-dependent. The significant interaction between fiber type and dosage indicates that increasing the fiber content does not necessarily lead to improved compressive performance. In contrast, although several fiber-reinforced mixtures exhibited numerically higher flexural strengths than the control, neither the one-way ANOVA nor the two-way ANOVA identified statistically significant effects of formulation, fiber type, dosage, or their interaction on flexural strength ($p > 0.05$). The flexural results should therefore be interpreted as indicating a favorable numerical tendency rather than a statistically demonstrated improvement. At higher fiber dosages, the observed variations in compressive strength may be associated with reduced workability and local fiber agglomeration, which can affect fiber dispersion and the homogeneity of the cementitious matrix [40,41].

3.4.3. Shrinkage Behavior

All fiber-reinforced concretes showed significant reductions in shrinkage throughout the measurement period (Table 9). At 7 days, the control recorded 390 μm/m; F2B3 (0.15%) achieved the lowest value of 98 μm/m, a reduction of 74.9%. F1B2 at 0.10% reduced 7-day shrinkage to 185 μm/m (−52.6%), confirming the effectiveness of the fiber network even at moderate dosages [40,41].

The significant reduction in early-age shrinkage observed across the fiber-reinforced mixtures may be associated with the restraining effect of the dispersed fiber network on volumetric deformation during cement hydration [40,41]. PP fibers may act as micro-reinforcement elements that help redistribute internal tensile stresses and delay microcrack development during early hydration stages [5,7,41]. The magnitude of this effect appears to depend on fiber dosage, geometry, and dispersion quality [7,17,41]. At higher dosages, fiber clustering and less uniform dispersion may limit the effectiveness of the reinforcing network and stress transfer [17,35,41]. The observed variability in shrinkage performance between fiber types further highlights the combined influence of fiber geometry, dosage, and dispersion quality. F2, with its uniform cylindrical cross-section and greater length, exhibited the lowest shrinkage at 0.15% among the investigated mixtures; this may be associated with a more effective fiber network and stress redistribution capacity, although these mechanisms were not directly quantified in the present study.

Table 9. Shrinkage (μm/m) of fiber-reinforced concrete at 2, 3, 5, and 7 days.

Fiber	Ref.	Dosage	2 d (μm/m)	3 d (μm/m)	5 d (μm/m)	7 d (μm/m)
Control	BN	0%	159 ± 0.6	194 ± 0.6	256 ± 0.6	390 ± 0.6
F1	F1B1	0.05%	133 ± 0.5	157 ± 0.6	208 ± 0.6	269 ± 0.7
	F1B2	0.10%	85 ± 0.4	111 ± 0.6	149 ± 0.6	185 ± 0.5
	F1B3	0.15%	59 ± 0.4	74 ± 0.4	133 ± 0.6	165 ± 0.5
F2	F2B1	0.05%	55 ± 0.4	86 ± 0.4	214 ± 0.6	271 ± 0.5
	F2B2	0.10%	46 ± 0.5	58 ± 0.4	82 ± 0.5	109 ± 0.4
	F2B3	0.15%	21 ± 0.4	36 ± 0.3	68 ± 0.4	98 ± 0.3
F5	F5B1	0.05%	59 ± 0.4	93 ± 0.3	129 ± 0.5	155 ± 0.5
	F5B2	0.10%	49 ± 0.4	76 ± 0.3	113 ± 0.5	148 ± 0.5
	F5B3	0.15%	46 ± 0.4	74 ± 0.3	91 ± 0.4	144 ± 0.5
F8	F8B1	0.05%	76 ± 0.4	176 ± 0.6	242 ± 0.6	348 ± 0.7
	F8B2	0.10%	39 ± 0.4	70 ± 0.4	155 ± 0.60	215 ± 0.7
	F8B3	0.15%	17 ± 0.4	48 ± 0.4	101 ± 0.4	194 ± 0.6

3.4.4. Water Absorption

The results are presented in Table 10 and Figure 4.

Table 10. Water absorption (%) of fiber-reinforced concrete at 2, 7, and 28 days.

Fiber	Ref.	Dosage	2 d * (%)	7 d * (%)	28 d * (%)	Change vs. Ctrl (28 d)
Control	BN	0%	5.89 ± 0.2	5.70 ± 0.3	4.49 ± 0.2	–
F1	F1B1	0.05%	6.73 ± 0.2	6.58 ± 0.3	4.94 ± 0.2	+10%
	F1B2	0.10%	6.79 ± 0.2	6.63 ± 0.3	5.14 ± 0.2	+14.5%
	F1B3	0.15%	7.08 ± 0.3	6.70 ± 0.3	5.38 ± 0.3	+19.8%
F2	F2B1	0.05%	5.96 ± 0.2	5.72 ± 0.3	4.56 ± 0.2	+1.6%
	F2B2	0.10%	6.02 ± 0.2	5.81 ± 0.3	4.71 ± 0.2	+4.9%
	F2B3	0.15%	6.18 ± 0.2	6.06 ± 0.3	4.82 ± 0.2	+7.3%
F5	F5B1	0.05%	6.55 ± 0.2	5.88 ± 0.4	4.63 ± 0.2	+3.1%
	F5B2	0.10%	6.60 ± 0.3	6.00 ± 0.4	4.78 ± 0.2	+6.5%
	F5B3	0.15%	6.78 ± 0.3	6.38 ± 0.4	5.08 ± 0.3	+13.1%
F8	F8B1	0.05%	6.33 ± 0.3	6.18 ± 0.4	4.65 ± 0.3	+3.6%
	F8B2	0.10%	6.55 ± 0.3	6.30 ± 0.4	5.01 ± 0.4	+11.6%
	F8B3	0.15%	6.71 ± 0.3	6.51 ± 0.4	5.36 ± 0.4	+19.4%

* The specimens were tested at 2, 7, and 28 days of age; these ages refer to the age at the beginning of the water absorption test, not to the duration of immersion.

Compared with the control concrete, water absorption increased with fiber incorporation, with the magnitude of the increase depending on both fiber type and dosage. At 0.10% fiber content, the increase remained relatively moderate for F2 and F5 (+4.9% and +6.5%, respectively), but was more pronounced for F1 and F8 (+14.5% and +11.6%). The highest increases were generally observed at a 0.15% dosage.

The observed increase in water absorption may be associated with localized modifications of the fiber–matrix interface and with changes in fiber dispersion within the cementitious matrix [7,41]. However, water absorption alone does not allow direct conclusions to be drawn regarding the connectivity of the overall pore network.

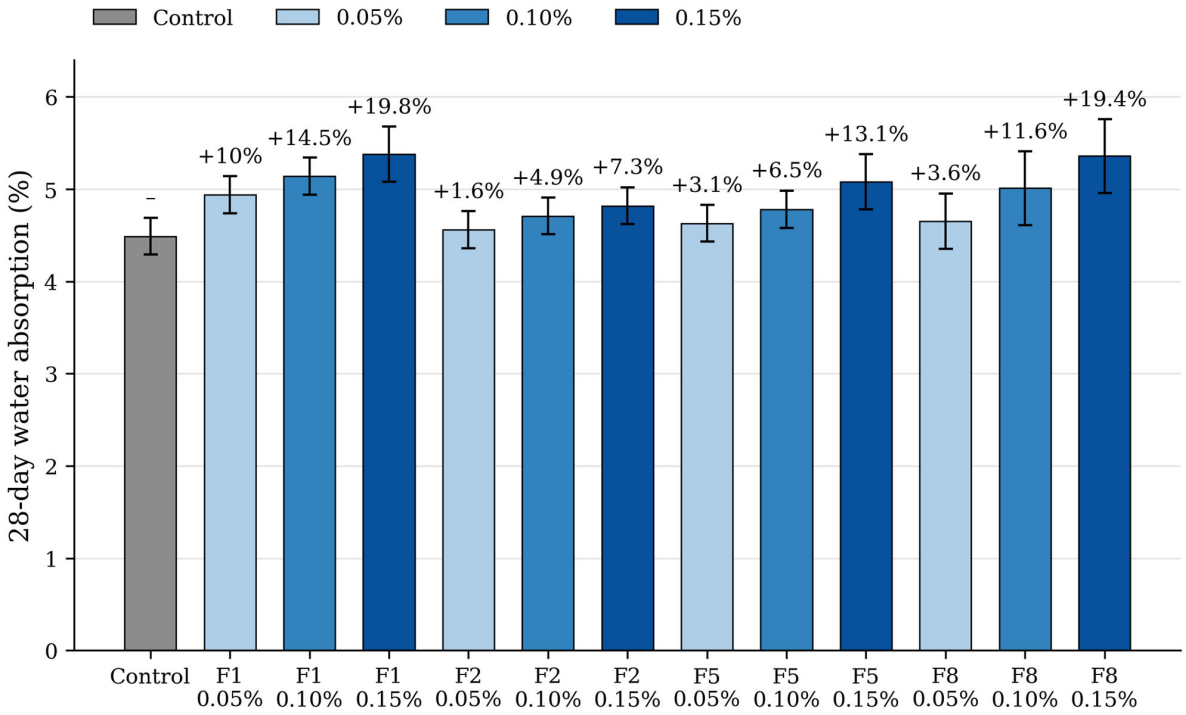

Figure 4. Water absorption (%) of fiber-reinforced concrete at 28 days.

The chloride diffusion coefficients and gas permeability measured after 90 days provide complementary transport-related information. The relatively low values obtained, particularly for F8, indicate favorable resistance to chloride and gas transport under the investigated conditions. However, these measurements do not establish a direct relationship between water absorption and pore-network connectivity, and the mechanisms governing the observed differences cannot be directly determined from the present measurements.

3.4.5. Selected Fiber Dosage

Across the investigated performance indicators, the 0.10% fiber dosage provided a favorable overall balance between fresh-state workability, mechanical performance, and shrinkage reduction within the investigated range. However, the response varied depending on fiber type and geometry, and no formal optimization procedure was performed. Therefore, 0.10% should be considered the selected dosage among the investigated levels rather than a mathematically determined or universally optimal dosage.

At higher dosages, particularly 0.15%, the benefits associated with fiber incorporation were accompanied in some mixtures by reduced workability and a greater tendency toward fiber clustering, which may affect fiber dispersion and stress transfer within the cementitious matrix [6,7,17,19].

Based on the comparative results obtained for the investigated dosage levels, 0.10% by mass of cement was selected for the detailed durability and microstructural investigations presented in the following sections. This selection reflects the overall experimental performance observed within the investigated range and does not imply that 0.10% represents a statistically optimal dosage or a universal optimum for recycled PP fiber-reinforced concrete.

3.5. Transport-Related Durability Indicators After 90 Days of Curing

3.5.1. Chloride Diffusion Coefficient

The resistance of the concrete mixtures to chloride ingress was evaluated after 90 days of curing by determining the apparent chloride diffusion coefficient in accordance with XP P18-462. The obtained results are presented in Figure 5.

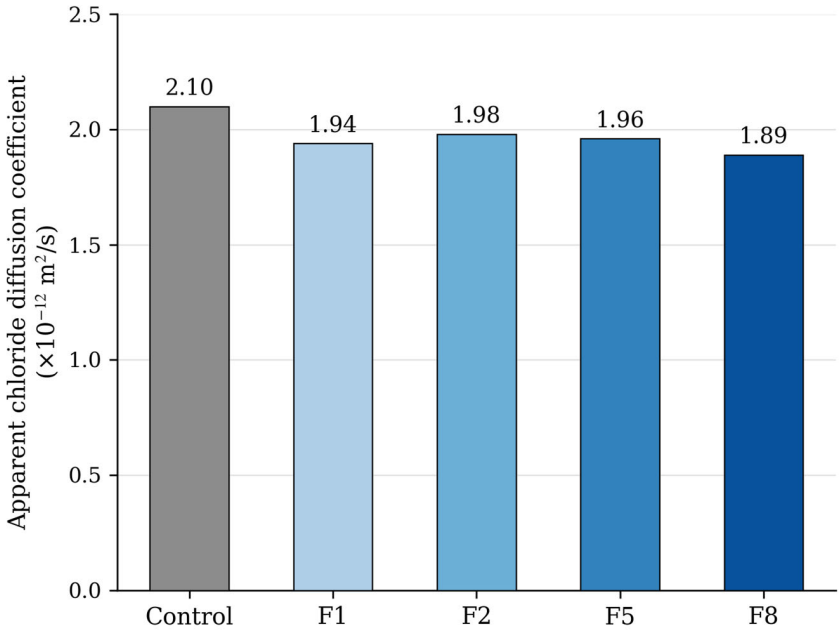

Figure 5. Apparent chloride diffusion coefficient of the investigated concrete mixtures.

All concrete mixtures exhibited relatively low apparent chloride diffusion coefficients, ranging from **1.89 × 10^{-12} to 2.10 × 10^{-12} m^2/s**, indicating a limited capacity for chloride ion transport through the hardened cementitious matrix. Compared with the control concrete, all fiber-reinforced mixtures exhibited slightly lower diffusion coefficients. Among the investigated formulations, the concrete reinforced with F8 fibers exhibited the lowest diffusion coefficient, whereas the highest value was recorded for the F2 mixture. Although the differences remain relatively small, the lower chloride diffusivity observed for F8 may indicate a greater resistance to chloride ingress under the investigated conditions.

3.5.2. Water Accessible Porosity

The water-accessible porosity of the concrete mixtures was determined after 90 days of curing according to NM 10.1.658. The results are summarized in Figure 6.

The measured porosity values of the fiber-reinforced mixtures ranged from 9.08% to 9.64%, indicating relatively low water-accessible porosity for all investigated concretes after 90 days of curing. The F8 mixture presented the lowest water-accessible porosity, while the highest value among the fiber-reinforced mixtures was measured for F5. The lower porosity observed for F8 is consistent with its reduced chloride diffusion coefficient and may be associated with differences in the accessibility and transport pathways of the pore network. Compared with the control concrete (10.8%), all fiber-reinforced mixtures exhibited lower water-accessible porosity. These results indicate that the incorporation of recycled textile fibers did not increase the accessible pore volume under the conditions of the test and may be associated with a relatively compact cementitious matrix in the investigated specimens.

It should be noted that the lower water-accessible porosity observed in the fiber-reinforced mixtures does not necessarily imply a corresponding decrease in water absorption. The two properties were determined using different test procedures and conditions and characterize different aspects of water uptake and pore accessibility. Therefore, the increase in water absorption reported in Section 3.4.4 and the lower water-accessible porosity observed after 90 days should not necessarily be interpreted as contradictory. A direct relationship between these two parameters cannot be established from the present measurements alone.

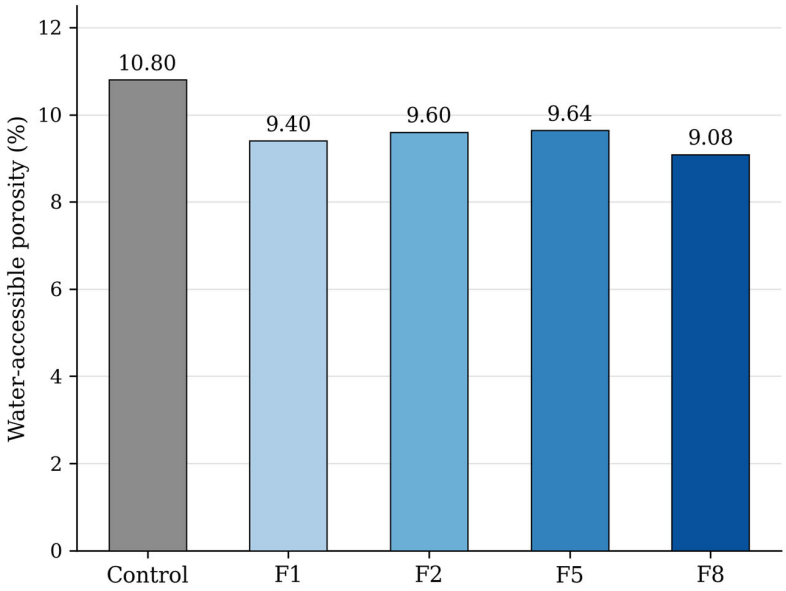

Figure 6. Water accessible porosity of the investigated concrete mixtures.

3.5.3. Apparent Gas Permeability

The apparent gas permeability of the concrete mixtures was measured after 90 days of curing in accordance with NM 10.1.442. The corresponding results are presented in Table 11.

Table 11. Apparent gas permeability of the investigated concrete mixtures.

Mixture	Control	F1	F2	F5	F8
Apparent gas permeability ($\times 10^{-18}$ m^2)	120	103	105	105	101

The apparent gas permeability values varied between 101 $\times$ 10^{-18} and 105 $\times$ 10^{-18} m^2. Once again, the F8 concrete exhibited the lowest permeability, whereas the highest values were obtained for the F2 and F5 mixtures. The reduced gas permeability indicates that the F8 formulation exhibited greater resistance to gas transport through the hardened matrix under the investigated conditions. This observation is consistent with the chloride diffusion and water-accessible porosity results and may be associated with differences in the accessibility and transport pathways of the pore network.

Taken together, the three transport-related durability indicators consistently identify the F8 formulation as the best-performing concrete among the investigated formulations after 90 days of curing. This mixture simultaneously exhibited the lowest apparent chloride diffusion coefficient, the lowest water-accessible porosity, and the lowest apparent gas permeability among the investigated formulations. Although the differences between mixtures remain moderate, the agreement between these three independent transport-related tests may indicate favorable transport characteristics of the F8 formulation. However, these results do not directly demonstrate a reduction in bulk pore-network connectivity, and quantitative pore-structure characterization would be required to confirm such a mechanism.

These findings are in good agreement with the SEM observations, which suggested a homogeneous fiber distribution and a relatively compact cementitious matrix with no significant interfacial voids surrounding the embedded fibers [36]. These localized observations are consistent with the favorable transport-related properties measured for the F8 formulation. However, the SEM observations are qualitative and limited to the analyzed regions; therefore, they cannot be considered direct evidence of changes in bulk pore-network connectivity or durability beyond the investigated transport-related properties at 90 days.

Overall, the combined mechanical, durability, and microstructural results indicate that the incorporation of recycled textile fibers can provide favorable concrete performance under the investigated conditions.

3.6. SEM-EDS Analysis

3.6.1. Recycled Textile Fiber

SEM observations of the recycled textile fiber F8 before its incorporation into the cementitious matrix are presented in Figure 7. F8 was selected for detailed SEM-EDS observation because it showed the most favorable overall mechanical performance among the investigated fiber types when incorporated into concrete. At low magnification, the fibers appear as elongated bundles with irregular dimensions, reflecting the heterogeneous nature of recycled textile waste. Higher magnification observations reveal that each bundle is composed of numerous fine filaments aligned along the longitudinal direction. The fibers exhibit a rough and irregular surface texture with longitudinal grooves, resulting in an increased specific surface area [17].

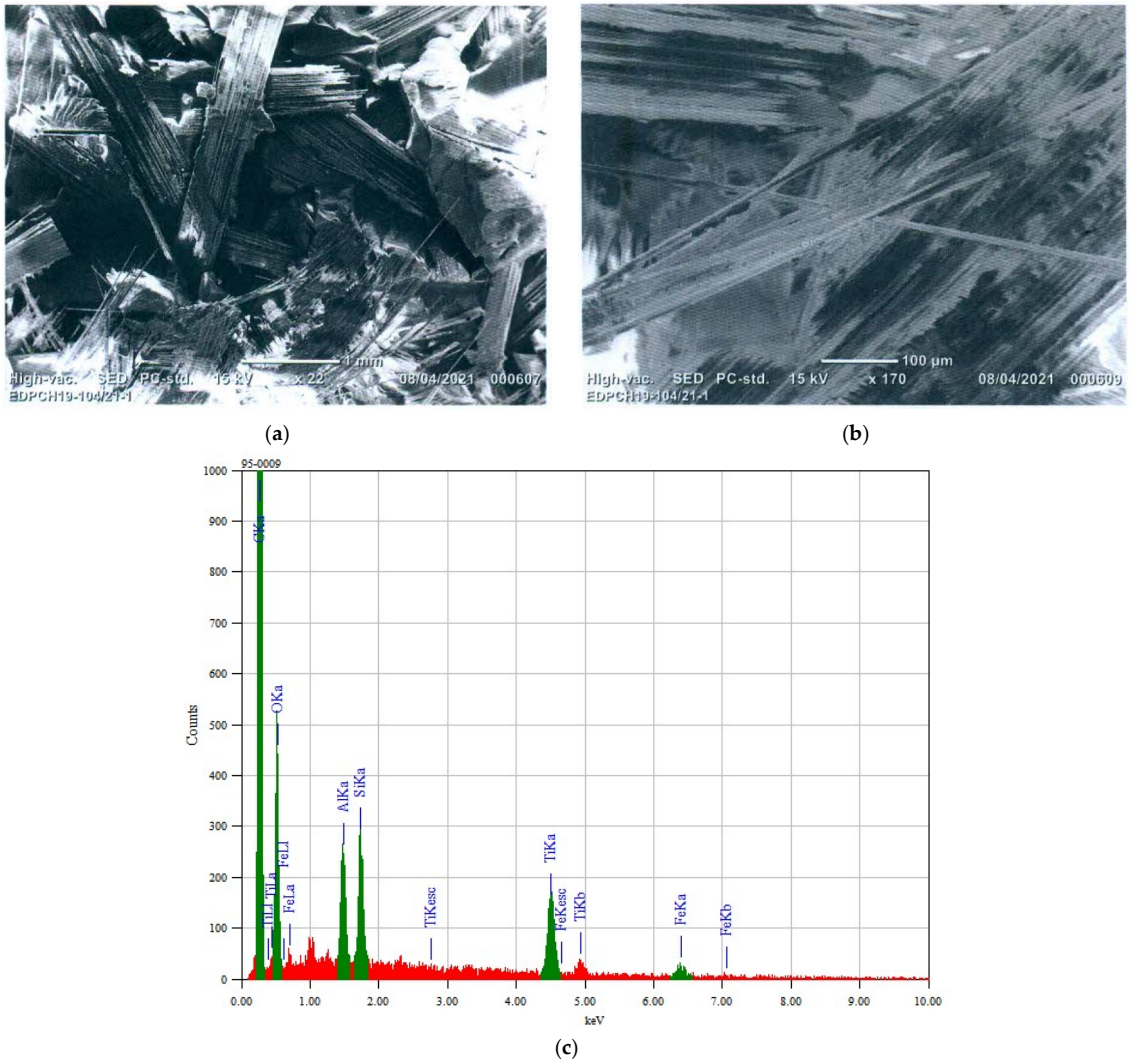

Figure 7. (**a**) Low-magnification SEM image illustrating the entangled structure of the recycled textile fiber F8 bundles (×22); (**b**) SEM image showing the fibrillated surface morphology of F8 (×170); (**c**) EDS spectrum of the recycled polypropylene fiber F8.

Such a multifilament morphology is expected to promote mechanical interlocking with the surrounding cement paste and may facilitate stress transfer between the fibers

and the cementitious matrix [7,19,21]. Despite this rough surface texture, no signs of severe degradation were observed, suggesting that the recycling process preserved the structural integrity of the fibers.

The corresponding EDS analysis (Figure 7c) confirms the polymeric nature of the recycled fibers, with carbon as the predominant element, accompanied by oxygen and minor amounts of titanium, silicon, aluminum and iron. The detected titanium is likely associated with titanium dioxide (TiO_2), commonly used as a pigment or delustering agent in textile manufacturing [42].

3.6.2. Fiber Reinforced Concrete

SEM observations of the concrete mixture F8B2, reinforced with 0.10% (by mass of cement) recycled polypropylene textile fibers (F8), are presented in Figure 8. This formulation was selected because it combined the highest compressive strength, one of the highest flexural strengths, and the most favorable transport-related durability properties among the investigated mixtures.

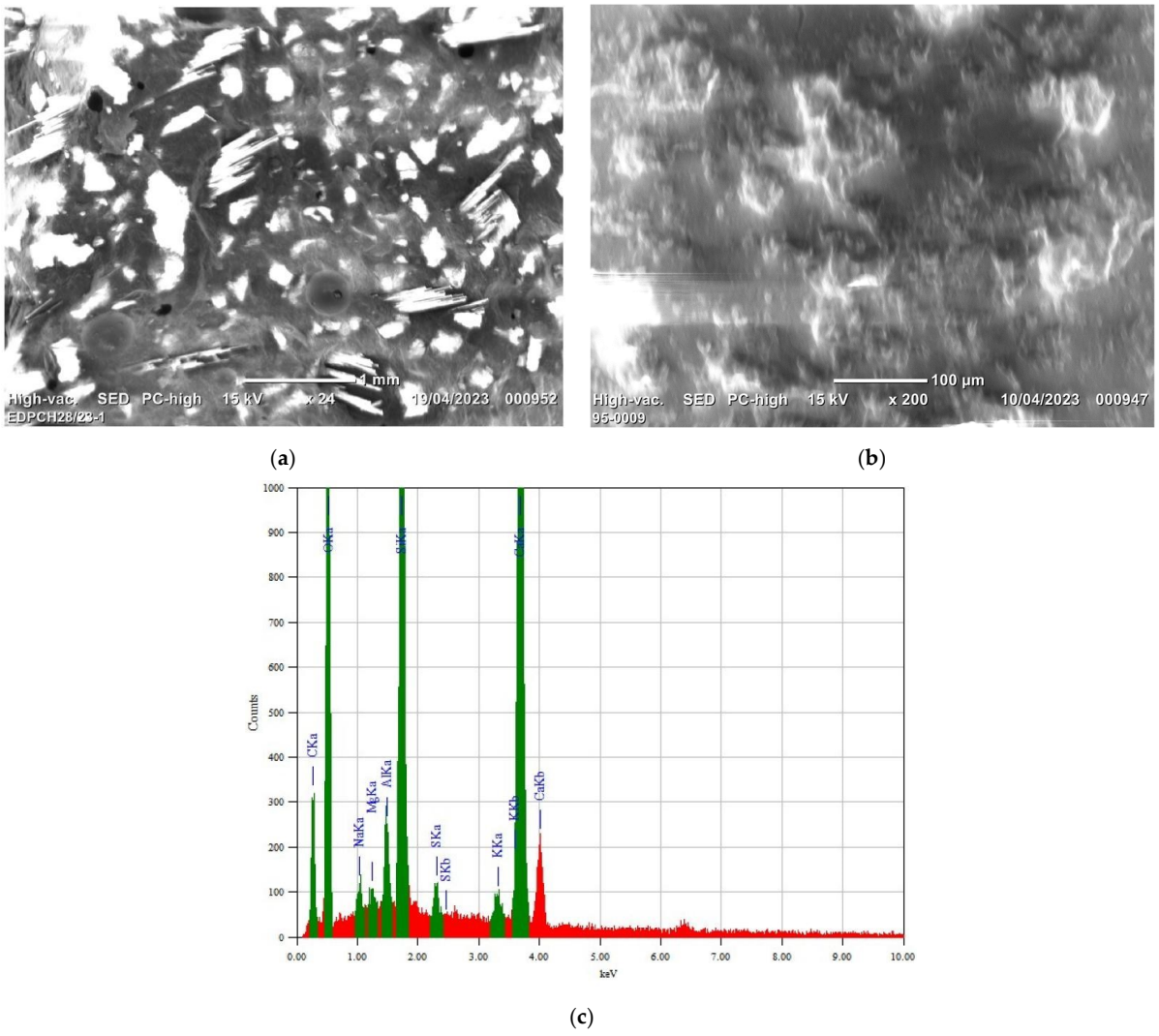

Figure 8. SEM-EDS micrographs of concrete reinforced with 0.10% recycled polypropylene textile fibers: (**a**) low-magnification image (×24) showing the distribution of the fibers within the cementitious matrix; (**b**) higher-magnification image (×200) illustrating the local morphology of the hardened cementitious matrix; (**c**) EDS spectrum acquired from the analyzed region, showing the predominant presence of silicon and calcium, together with a distinct carbon peak and minor amounts of sodium, magnesium, aluminum, sulfur, and potassium.

At low magnification, the fibers appear distributed throughout the analyzed cementitious matrix without evidence of large-scale fiber agglomeration. Such an observation is consistent with satisfactory fiber incorporation within the investigated region [5,7]. Most fibers appear embedded in the hardened matrix, indicating their incorporation into the cementitious matrix [5].

At higher magnification, the cementitious matrix appears relatively dense within the analyzed region, with limited visible porosity at the investigated scale. No obvious major cracks are observed within the analyzed region. Although the present observations remain qualitative and limited to the investigated regions of the specimen, they provide complementary information on the local microstructural appearance of the F8B2 concrete.

The EDS spectrum acquired from the cementitious matrix is dominated by silicon and calcium, together with a distinct carbon peak and smaller amounts of sodium, magnesium, aluminum, sulfur, and potassium. This elemental composition is typical of hydrated Portland cement systems and is consistent with the presence of calcium silicate hydrate (C–S–H), portlandite (CH), and other cement hydration products. The detection of aluminum and sulfur may be associated with sulfate-bearing hydration products (e.g., ettringite or monosulfoaluminate), whereas the alkali elements (Na and K) are typically associated with the cementitious binder. Given the localized nature of point EDS analysis, a minor contribution from adjacent fine aggregate particles cannot be entirely excluded. Although EDS does not directly identify hydration phases, the observed elemental composition is fully consistent with that expected for hydrated Portland cement paste.

Overall, the SEM observations indicate a relatively dense cementitious matrix in which the recycled textile fibers appear to be homogeneously dispersed and adequately embedded, while the EDS analysis confirms the characteristic elemental composition of hydrated Portland cement paste. Although qualitative in nature and limited to the analyzed regions, these observations are consistent with the experimentally measured transport properties, including the low chloride diffusion coefficients, low water-accessible porosity, and low apparent gas permeability observed for the F8 formulation. However, these localized observations do not provide a systematic quantitative assessment of fiber dispersion, agglomeration, fiber–matrix interfacial transition zones, or bulk pore-network connectivity. Therefore, the observed microstructural features may be associated with the favorable transport-related properties measured for F8, while quantitative pore-structure characterization would be required to confirm such a relationship.

4. General Discussion

4.1. Influence of Fiber Geometry on the Performance of Recycled Textile Fiber

Although all investigated fibers consisted of 100% polypropylene, the differences in their observed performance may be related, among other factors, to their geometrical and morphological characteristics, since their bulk polymeric composition was essentially identical. Fiber diameter, length, aspect ratio, and cross-sectional morphology can influence fiber–matrix interaction, stress transfer, crack-bridging capacity, and dispersion within cementitious mixtures [7,17,21,37]. These parameters are therefore particularly relevant for recycled textile fibers, whose geometrical variability is inherent to the waste-recycling process.

For polypropylene fibers, which have limited chemical affinity with cementitious matrices, stress transfer is expected to involve mechanical interlocking, frictional resistance, and crack bridging rather than chemical bonding alone. The rough and fibrillated surface observed by SEM for F8, together with its multifilament structure, may increase mechanical interaction with the surrounding cementitious matrix. However, these observations remain qualitative, and the relative contributions of surface morphology, friction, and mechanical

anchorage cannot be separated without dedicated interfacial characterization or single-fiber pull-out testing.

The observed differences between fiber types can therefore be interpreted as the combined result of geometry, morphology, and dispersion rather than geometry alone. Higher aspect ratios may improve crack bridging and mechanical anchorage, whereas irregular cross-sectional morphologies, such as those observed for F5, may lead to less uniform stress transfer [7,17,21,43]. The longer F2 fibers, for example, may have favored the formation of a more continuous reinforcing network and consequently contributed to its stronger shrinkage-control effect at the mortar scale. However, this effect cannot be attributed to fiber length alone because diameter, cross-sectional morphology, surface condition, and dispersion also differed among the investigated fibers.

At the concrete scale, the presence of coarse aggregates introduces an additional constraint on fiber dispersion and workability. Consequently, increasing fiber dosage may enhance crack restraint but simultaneously increase internal friction and the risk of local fiber clustering, potentially limiting the efficiency of stress transfer [7,13,21,35]. This interaction explains why 0.10% by mass of cement was selected for further concrete investigation: within the investigated range, it provided a favorable overall balance between workability, mechanical response, and shrinkage reduction for the selected formulations, rather than representing a universal optimum.

From a practical perspective, the results indicate that screening heterogeneous recycled textile fibers before concrete incorporation is important because fiber geometry and morphology can strongly affect their processability and reinforcing efficiency. Nevertheless, the present study did not quantify fiber–matrix bond strength, surface chemistry, or the statistical representativeness of fiber dispersion. These limitations should be considered when interpreting the mechanisms proposed above, and future work involving pull-out testing and quantitative microstructural characterization would help establish more directly the relationship between recycled fiber characteristics and composite performance.

4.2. Microstructure-Durability Relationship

The durability results obtained after 90 days are in agreement with the microstructural observations performed by SEM–EDS. The selected concrete mixture exhibited the lowest chloride diffusion coefficient, water-accessible porosity, and apparent gas permeability, while SEM observations revealed a relatively homogeneous and compact cementitious matrix with well-dispersed fibers and no obvious interfacial defects [44,45]. Although SEM observations remain qualitative, the agreement between transport properties and microstructural evidence suggests that the incorporation of recycled textile fibers did not adversely affect matrix integrity and may have contributed to the development of a less permeable cementitious microstructure [1,36].

4.3. Practical Implications and Limitations

The dosage selected for further investigation in this study (0.10% by mass of cement) provided a favorable overall balance among the investigated performance indicators and is within the dosage range commonly reported for polypropylene fiber-reinforced cementitious composites [21,41]. Likewise, the reductions in shrinkage and the improvements in flexural performance obtained with the recycled fibers are broadly comparable to those reported for commercially manufactured polypropylene fibers, indicating that recycled textile waste has potential for use as a reinforcement in cementitious composites [7,35,41].

Fiber dispersion represents a critical processing parameter when incorporating heterogeneous recycled textile fibers into cementitious mixtures. In the present study, the progressive reduction in workability and the increased tendency for fiber agglomeration

observed at higher dosages demonstrated the importance of controlling fiber content and mixing conditions. Accordingly, concrete mixtures were restricted to a fiber dosage of 0.05–0.15% by mass of cement, while higher contents were excluded because of the observed non-uniform dispersion. The slump results further confirmed the reduction in workability with increasing fiber content. These findings indicate that adequate dispersion of heterogeneous recycled textile fibers requires controlled fiber dosage, gradual fiber addition, sufficient mixing, and preliminary screening based on fiber length and morphology. In this regard, the 3 mm lower length threshold applied during fiber screening, while supported by published criteria for minimum embedment length and workability preservation [7,17,19,21], was not experimentally validated within this study. Future work should quantify the fresh-state and hardened-state effects of including sub-3 mm fractions—including their potential role as micro-reinforcement in a hybrid fiber system for multi-scale crack control [5,7,19]—to refine this criterion for heterogeneous industrial waste streams. It should be noted that the exclusion of fibers shorter than 3 mm precludes any potential multi-scale reinforcement effect. Hybrid fiber systems combining micro- and macro-length fibers are well-documented in the literature as an effective strategy for controlling both early-stage microcracks and propagating macrocracks [5,19,21,37]. The incorporation of the fine fraction of recycled textile fibers as a micro-reinforcement component represents a promising avenue for future research and would allow fuller valorization of the heterogeneous waste stream.

The SEM observations of the selected F8B2 mixture showed a generally homogeneous distribution of fibers without extensive visible agglomeration. Nevertheless, because SEM observations were performed on localized regions, they should be considered qualitative and cannot be regarded as statistically representative of the entire concrete volume.

Beyond the mechanical benefits, the experimental workflow—including systematic fiber screening, mortar-scale assessment, and concrete-scale validation—provides a practical framework for the valorization of industrial textile waste. Considering the significant quantities of pre-consumer textile waste generated by the Moroccan textile industry, this approach represents a promising strategy for promoting circular economy principles while contributing to the valorization of industrial textile waste within a circular economy framework [14,15].

Unlike most previous studies, which investigated a single commercial fiber type, the present work applies a systematic screening approach to heterogeneous recycled textile fibers prior to their incorporation into cementitious composites. This approach facilitates the selection of representative fibers for cementitious applications and provides a rational framework for the sustainable valorization of heterogeneous industrial textile waste.

Despite these encouraging results, the present study has several limitations. The durability assessment was limited to 90 days of curing and focused on transport-related properties under laboratory conditions. Additional investigations are required to evaluate the long-term performance of recycled fiber-reinforced concrete under more aggressive environmental exposures, including freeze–thaw cycles, sulfate attack, carbonation, and prolonged chloride exposure. Furthermore, complementary studies on fiber pull-out behavior, together with advanced characterization of the fiber–matrix interfacial transition zone using techniques such as scanning electron microscopy at higher magnification, micro-computed tomography (μCT), or nanoindentation, would provide a deeper understanding of the fiber–matrix interaction and reinforcement mechanisms.

A further consideration concerns the long-term behavior of recycled polypropylene fibers within the cementitious matrix. Because PP is a viscoelastic polymer, fiber deformation and creep may occur under sustained loading, while insufficient interfacial anchorage may promote progressive fiber pull-out. These mechanisms may limit the contribution of recycled PP fibers to long-term load transfer, particularly under sustained structural

stresses. In the present study, the reinforcement mechanism was evaluated indirectly through flexural strength, shrinkage, and microstructural observations; dedicated fiber pull-out and long-term creep tests were not performed. Accordingly, the present results should not be interpreted as evidence of the long-term structural load-bearing capacity of the recycled PP fibers. Future investigations should include single-fiber pull-out tests, bond-slip characterization, and sustained-load creep tests. From an engineering perspective, fiber length, aspect ratio, cross-sectional morphology, and dosage should be optimized to improve mechanical anchorage while avoiding excessive fiber contents that may promote agglomeration. Another limitation concerns the mechanical characterization of the individual recycled fibers. Although tensile strength and elastic modulus are relevant parameters for assessing the intrinsic reinforcing potential of fibers, these properties were not experimentally determined in the present study because the specialized equipment required for tensile testing of individual textile fibers was not available in the laboratory. Accordingly, no values were estimated or assumed. The fiber characterization was instead based on the experimentally determined geometrical, morphological, chemical, and physical properties, while the reinforcing performance was evaluated through the mechanical response of the cementitious composites. Future studies should include tensile testing of individual recycled fibers to further establish the relationship between their intrinsic mechanical properties and the performance of the resulting composites.

For applications involving significant sustained structural loading, recycled PP fibers should preferably be considered as complementary crack-control reinforcement rather than as a substitute for conventional structural reinforcement unless their long-term performance has been specifically demonstrated.

5. Conclusions

This study investigated the feasibility of valorizing recycled polypropylene fibers derived from Moroccan industrial textile waste as reinforcement for cementitious materials through a multi-scale experimental approach involving fiber characterization, mortar-scale assessment, concrete evaluation, transport-related durability indicators, and microstructural characterization.

The main findings can be summarized as follows.

Morphological screening reduced an initial set of thirteen recycled textile fiber types to four representative fibers based on their geometrical and morphological characteristics. Although all selected fibers consisted of 100% polypropylene, significant differences in diameter, length, aspect ratio, and cross-sectional morphology were observed. These variations, together with differences in surface morphology, fiber condition, and dispersion behavior, may contribute to the differences observed in cementitious performance. However, the relative contribution of these factors cannot be quantitatively separated based on the present experimental characterization.

Mechanical performance was influenced by both fiber dosage and fiber characteristics. Fiber incorporation significantly affected compressive strength, although the magnitude and direction of the effect varied depending on fiber type and dosage. In contrast, flexural strength showed a favorable numerical tendency, with improvements of up to 8.2% recorded for selected fiber types and dosages compared with the reference mixture; however, these differences were not statistically significant at the 95% confidence level. The magnitude and direction of the mechanical response varied depending on fiber type and dosage, suggesting that the observed performance may result from the combined effects of fiber geometry, surface characteristics, intrinsic fiber properties, and dispersion. Among the investigated dosage levels, 0.10%, by mass, of cement provided a favorable overall balance for selected formulations, particularly F8, and was therefore selected for subsequent durability and microstructural investigations. However, this dosage cannot be considered a universal

optimum. The statistically significant fiber type × dosage interaction ($F = 8.454$, $p < 0.001$) indicates that the effect of fiber dosage on compressive strength depended on fiber type and, consequently, could not be generalized across the investigated fiber formulations.

The most pronounced effect was observed for early-age shrinkage. Shrinkage was reduced by up to 75% compared with the reference mixture, demonstrating the potential of recycled polypropylene fibers to mitigate early-age volumetric deformation under the investigated conditions. The magnitude of shrinkage reduction varied with fiber type and dosage, suggesting that differences in fiber geometry, surface condition, and dispersion may contribute to the observed response. However, the individual contribution of these parameters could not be established from the present experimental data.

Transport-related durability indicators evaluated after 90 days of water curing showed relatively low apparent chloride diffusion coefficients, water-accessible porosity, and apparent gas permeability for the investigated mixtures. Among them, the F8 formulation exhibited the most favorable combination of these transport-related properties. These results may be associated with favorable characteristics of the accessible pore network; however, the present measurements do not directly demonstrate changes in bulk pore-network connectivity or long-term durability.

SEM–EDS observations of the selected F8B2 mixture showed that the recycled fibers appeared relatively uniformly distributed and adequately embedded within the analyzed regions of the cementitious matrix. The observed matrix appeared relatively dense at the investigated scale, with no obvious major defects in the analyzed regions. However, these observations are qualitative and localized and therefore cannot be considered direct evidence of differences in bulk microstructure, pore-network connectivity, or matrix compactness among the investigated mixtures.

Overall, the systematic experimental screening and validation framework, combining fiber screening, mortar-scale assessment, concrete evaluation, transport-related durability indicators, and microstructural characterization, demonstrates the potential of heterogeneous recycled polypropylene textile fibers for use as reinforcement in cement-based materials under the investigated experimental conditions. The results particularly highlight their potential for reducing early-age shrinkage and for contributing to the valorization of industrial textile waste within a circular-economy framework, while broader environmental benefits cannot be established without a dedicated life-cycle assessment.

Future research should investigate the long-term durability of recycled fiber-reinforced concrete under aggressive environmental conditions, including freeze–thaw cycles, sulfate attack, carbonation, wetting–drying cycles, and prolonged chloride exposure. Additional studies focusing on fiber pull-out behavior, tensile strength and elastic modulus of individual recycled fibers, quantitative pore-structure characterization, comparison with virgin and commercial PP fibers, and life-cycle assessment would help further clarify the mechanisms governing performance and assess the broader environmental implications and potential for large-scale application of recycled textile fibers in cement-based materials.

Supplementary Materials: The following supporting information can be downloaded at: https://www.mdpi.com/article/10.3390/fib14090103/s1, Table S1: Geometrical and physical characteristics of all thirteen initial recycled PP fiber types investigated during the screening stage, together with their aspect ratio, selection status, and reasons for exclusion or selection. Selected fibers (F1, F2, F5, F8) are highlighted in green. References [46–48] are cited in the supplementary materials.

Author Contributions: Conceptualization, I.H. and A.N.; methodology, I.H. and A.N.; validation, I.H., A.N., and R.E.; formal analysis, I.H.; investigation, I.H.; resources, O.B.; data curation, O.B.; writing—original draft preparation, I.H.; writing—review and editing, A.N. and R.E.; visualization, I.H.; supervision, R.E.; project administration, I.H. All authors have read and agreed to the published version of the manuscript.

Funding: This research received no external funding.

Institutional Review Board Statement: Not applicable.

Informed Consent Statement: Not applicable.

Data Availability Statement: The data presented in this study are available in the article.

Conflicts of Interest: The authors declare no conflicts of interest.

Abbreviations

The following abbreviations are used in this manuscript:

PP	Polypropylene
FRCC	Fiber-reinforced cementitious composites
SEM-EDS	Scanning electron microscopy with energy dispersive X-ray spectroscopy
C-S-H	Calcium silicate hydrate
ITZ	ITZ

References

1. Mehta, P.K.; Monteiro, P.J.M. *Concrete: Microstructure, Properties, and Materials*, 4th ed.; McGraw-Hill Education: New York, NY, USA, 2014.
2. Altoubat, S.A.; Lange, D.A. Creep, shrinkage, and cracking of restrained concrete at early age. *ACI Mater. J.* **2001**, *98*, 323–331. [CrossRef] [PubMed]
3. Ahmad, J.; Burduhos-Nergis, D.D.; Arbili, M.M.; Alogla, S.M.; Majdi, A.; Deifalla, A.F. A Review on Failure Modes and Cracking Behaviors of Polypropylene Fibers Reinforced Concrete. *Buildings* **2022**, *12*, 1951. [CrossRef]
4. Bertelsen, I.M.G.; Ottosen, L.M.; Fischer, G. Influence of Fibre Characteristics on Plastic Shrinkage Cracking in Cement-Based Materials: A Review. *Constr. Build. Mater.* **2020**, *230*, 116769. [CrossRef]
5. Bentur, A.; Mindess, S. *Fibre Reinforced Cementitious Composites*, 2nd ed.; Taylor & Francis: London, UK, 2007.
6. Kakooei, S.; Akil, H.M.; Jamshidi, M.; Rouhi, J. The effects of polypropylene fibers on the properties of reinforced concrete structures. *Constr. Build. Mater.* **2012**, *27*, 73–77. [CrossRef]
7. Banthia, N.; Gupta, R. Influence of polypropylene fiber geometry on plastic shrinkage cracking in concrete. *Cem. Concr. Res.* **2006**, *36*, 1263–1267. [CrossRef]
8. Sivakumar, A.; Santhanam, , M. Mechanical properties of high strength concrete reinforced with metallic and non-metallic fibres. *Cem. Concr. Compos* **2007**, *29*, 603–608.
9. Kos, Ž.; Kroviakov, S.; Kryzhanovskyi, V.; Hedulian, D. Strength, Frost Resistance, and Resistance to Acid Attacks on Fiber-Reinforced Concrete for Industrial Floors and Road Pavements with Steel and Polypropylene Fibers. *Materials* **2022**, *15*, 8339. [CrossRef] [PubMed]
10. Kroviakov, S.; Kryzhanovskyi, V.; Shymchenko, P.; Aksyonova, I. Multi-Objective Optimization of Rigid Pavement Concrete Using Industrial By-Products and Polypropylene Fibers. *Modelling* **2026**, *7*, 52. [CrossRef]
11. Spadea, S.; Farina, I.; Fraternali, F. Recycled Nylon Fibers as Cement Mortar Reinforcement. *Constr. Build. Mater.* **2015**, *80*, 200–209. [CrossRef]
12. Pelisser, F.; Montedo, O.R.K.; Gleize, P.J.P.; Roman, H.R. Mechanical Properties of Recycled PET Fibers in Concrete. *Mater. Res.* **2012**, *15*, 679–686. [CrossRef]
13. International Energy Agency (IEA). *Net Zero Roadmap: A Global Pathway to Keep the 1.5 °C Goal in Reach*; IEA: Paris, France, 2023.
14. Textile Exchange. *Preferred Fiber & Materials Market Report 2022*; Textile Exchange: Lamesa, TX, USA, 2022.
15. Tran, N.P.; Gunasekara, C.; Law, D.W.; Houshyar, S.; Setunge, S.; Cwirzen, A. Comprehensive Review on Sustainable Fiber Reinforced Concrete Incorporating Recycled Textile Waste. *J. Sustain. Cem.-Based Mater.* **2022**, *11*, 28–42. [CrossRef]
16. Hattab, I.; El Kacmi, R.; Boudouch, O. A Circular Economy Approach to Cement Production: Integrating Untreated Moroccan EAF Steel Slag for Performance and Sustainability. *Buildings* **2026**, *16*, 2661. [CrossRef]
17. Małek, M.; Jackowski, M.; Łasica, W.; Kadela, M. Characteristics of Recycled Polypropylene Fibers as an Addition to Concrete Fabrication Based on Portland Cement. *Materials* **2020**, *13*, 1827. [CrossRef] [PubMed]
18. Yin, S.; Tuladhar, R.; Riella, J.; Chung, D.; Collister, T.; Combe, M.; Sivakugan, N. Comparative Evaluation of Virgin and Recycled Polypropylene Fibre Reinforced Concrete. *Constr. Build. Mater.* **2016**, *114*, 134–141. [CrossRef]
19. Yin, S.; Tuladhar, R.; Shi, F.; Combe, M.; Collister, T.; Sivakugan, N. Use of Macro Plastic Fibres in Concrete: A Review. *Constr. Build. Mater.* **2015**, *93*, 180–188. [CrossRef]

20. *NF EN ISO 1833-1:2020*; Textiles—Quantitative Chemical Analysis—Part 1: General Principles of Testing. Association Française de Normalisation (AFNOR): Paris, France, 2020.
21. Afroughsabet, V.; Biolzi, L.; Ozbakkaloglu, T. High-performance fiber-reinforced concrete: A review. *J. Mater. Sci.* **2016**, *51*, 6517–6551.
22. *NM 10.1.005*; Hydraulic Binders—Test Methods. Service de Normalisation Industrielle Marocaine (SNIMA): Rabat, Morocco, 2008.
23. Dreux, G.; Festa, J. *Nouveau Guide du Béton et de ses Constituants*, 8th ed.; Eyrolles: Paris, France, 1998.
24. de Larrard, F. *Concrete Mixture Proportioning: A Scientific Approach*; E & FN Spon: London, UK, 1999.
25. *NM 10.1.061:2008*; Essai Pour béton Frais—Essai d'affaissement. Service de Normalisation Industrielle Marocaine (SNIMA): Rabat, Morocco, 2008.
26. *NM 10.1.051*; Concrete—Determination of Compressive Strength of Specimens. Moroccan Standards Institute: Rabat, Morocco, 2008.
27. *NM 10.1.050*; Concrete—Determination of Flexural Strength of Specimens. Moroccan Standards Institute: Rabat, Morocco, 2008.
28. *NF P 18-427:1996*; Béton—Détermination des Variations Dimensionnelles Entre Deux Faces Opposées D'éprouvettes de Béton Durci. Association Française de Normalisation (AFNOR): Paris, France, 1996.
29. *EN 13369:2013*; Common Rules for Precast Concrete Products. European Committee for Standardization (CEN): Brussels, Belgium, 2013.
30. Goldstein, J.I.; Newbury, D.E.; Michael, J.R.; Ritchie, N.W.M.; Scott, J.H.J.; Joy, D.C. *Scanning Electron Microscopy and X-Ray Microanalysis*, 4th ed.; Springer: New York, NY, USA, 2018.
31. *XP P18-462:2012*; Essai sur Béton Durci—Essai Accéléré de Migration des Ions Chlorure en Régime Non-Stationnaire—Détermination du Coefficient de Diffusion Apparent des Ions Chlorure. Association Française de Normalisation (AFNOR): Paris, France, 2012.
32. *NM 10.1.658:2021*; Béton—Essai pour béton Durci—Essai de Porosité et de Masse Volumique. Institut Marocain de Normalisation (IMANOR): Rabat, Morocco, 2021.
33. *NM 10.1.442:2021*; Bétons—Essai de Perméabilité aux gaz sur Béton Durci. Institut Marocain de Normalisation (IMANOR): Rabat, Morocco, 2021.
34. Osswald, T.A.; Menges, G. *Materials Science of Polymers for Engineers*, 3rd ed.; Hanser Publishers: Munich, Germany, 2012.
35. Bolat, H.; Sihoglu, S.; Turk, G. Effects of polypropylene fiber reinforcement on physical and mechanical properties of concrete. *Compos. Part B Eng.* **2014**, *57*, 166–171.
36. Ramezanianpour, A.A.; Esmaeili, M.; Ghahari, S.A.; Najafi, M.H. Laboratory study on the effect of polypropylene fiber on durability, and physical and mechanical characteristic of concrete for application in sleepers. *Constr. Build. Mater.* **2013**, *44*, 411–418. [CrossRef]
37. Yoo, D.Y.; Yoon, Y.S. A Review on structural behavior, design, and application of ultra-high-performance fiber-reinforced concrete. *Int. J. Concr. Struct. Mater.* **2016**, *10*, 125–142. [CrossRef]
38. Song, P.S.; Hwang, S. Mechanical properties of high-strength steel fiber-reinforced concrete. *Constr. Build. Mater.* **2004**, *18*, 669–673. [CrossRef]
39. Hsie, M.; Tu, C.; Song, P.S. Mechanical properties of polypropylene hybrid fiber-reinforced concrete. *Mater. Sci. Eng. A* **2008**, *494*, 153–157. [CrossRef]
40. Neville, A.M. *Properties of Concrete*, 5th ed.; Pearson Education: Harlow, UK, 2011.
41. Latifi, M.R.; Biricik, Ö.; Mardani Aghabaglou, A. Effect of the Addition of Polypropylene Fiber on Concrete Properties. *J. Adhes. Sci. Technol.* **2022**, *36*, 345–369. [CrossRef]
42. Hladik, J.; Reznickova, A.; Kormunda, M.; Slepicka, P. Titanium dioxide nanoparticles in textile applications: A review of preparation methods, properties, and functionalization. *Nanomaterials* **2021**, *11*, 2920.
43. Kim, D.J.; Park, S.H.; Ryu, G.S.; Koh, K.T. Comparative flexural behavior of hybrid ultra high performance fiber reinforced concrete with different macro fibers. *Constr. Build. Mater.* **2011**, *25*, 4144–4155. [CrossRef]
44. Scrivener, K.L.; Crumbie, A.K.; Laugesen, P. The interfacial transition zone (ITZ) between cement paste and aggregate in concrete. *Interface Sci.* **2004**, *12*, 411–421. [CrossRef]
45. Diamond, S. The microstructure of cement paste and concrete: A visual primer. *Cem. Concr. Compos.* **2004**, *26*, 919–933. [CrossRef]
46. Lauff, P.; Pugacheva, P.; Rutzen, M.; Weiß, U.; Fischer, O.; Volkmer, D.; Peter, M.A.; Grosse, C.U. Evaluation of the Behavior of Carbon Short Fiber Reinforced Concrete (CSFRC) Based on a Multi-Sensory Experimental Investigation and a Numerical Multiscale Approach. *Materials* **2021**, *14*, 7005. [CrossRef] [PubMed]
47. Tanaka, Y.; Hashimoto, O.; Sakamoto, J.; Nishi, K. Fiber Reinforced Cement Based Mixed Material. U.S. Patent 9,145,337, 29 September 2015. Available online: https://patents.google.com/patent/US9145337B2/en (accessed on 22 August 2026).
48. Salehi, A.; Asadollahfardi, G.; Mafakheri, S.; Homami, P.; Akbardoost, J.; Soleymani Tushmanlo, H.; Soleymani Tushmanlo, A. Impact of Propylene Fibers and Industrial Wastewater on the Properties of Self-Compacting Concrete. *Sci. Rep.* **2025**, *15*, 29201. [CrossRef]

Disclaimer/Publisher's Note: The statements, opinions and data contained in all publications are solely those of the individual author(s) and contributor(s) and not of MDPI and/or the editor(s). MDPI and/or the editor(s) disclaim responsibility for any injury to people or property resulting from any ideas, methods, instructions or products referred to in the content.